



HAL
open science

Membrane proteocomplexome of *Campylobacter jejuni* using 2-D blue native/SDS-PAGE combined to bioinformatics analysis

Alizée Guérin, Sheiam Sulaeman, Laurent Coquet, Armelle Ménard,
Frédérique Barloy-Hubler, Emmanuelle Dé, Odile Tresse

► To cite this version:

Alizée Guérin, Sheiam Sulaeman, Laurent Coquet, Armelle Ménard, Frédérique Barloy-Hubler, et al.. Membrane proteocomplexome of *Campylobacter jejuni* using 2-D blue native/SDS-PAGE combined to bioinformatics analysis. *Frontiers in Microbiology*, 2020, 11, 10.3389/fmicb.2020.530906 . hal-03765916

HAL Id: hal-03765916

<https://hal.inrae.fr/hal-03765916>

Submitted on 14 Mar 2023

HAL is a multi-disciplinary open access archive for the deposit and dissemination of scientific research documents, whether they are published or not. The documents may come from teaching and research institutions in France or abroad, or from public or private research centers.

L'archive ouverte pluridisciplinaire **HAL**, est destinée au dépôt et à la diffusion de documents scientifiques de niveau recherche, publiés ou non, émanant des établissements d'enseignement et de recherche français ou étrangers, des laboratoires publics ou privés.



Distributed under a Creative Commons Attribution 4.0 International License



HAL
open science

Membrane proteocomplexome of *Campylobacter jejuni* using 2-D blue native/SDS-PAGE combined to bioinformatics analysis

Odile Tresse, Alizée Guérin, Sheiam Sulaeman, Laurent Coquet, Armelle
Menard, Frédérique Barloy-Hubler, Emmanuelle Dé

► To cite this version:

Odile Tresse, Alizée Guérin, Sheiam Sulaeman, Laurent Coquet, Armelle Menard, et al.. Membrane proteocomplexome of *Campylobacter jejuni* using 2-D blue native/SDS-PAGE combined to bioinformatics analysis. *Frontiers in Microbiology*, 2020, 10.3389/fmicb.2020.530906 . hal-02995535

HAL Id: hal-02995535

<https://hal.science/hal-02995535>

Submitted on 9 Nov 2020

HAL is a multi-disciplinary open access archive for the deposit and dissemination of scientific research documents, whether they are published or not. The documents may come from teaching and research institutions in France or abroad, or from public or private research centers.

L'archive ouverte pluridisciplinaire **HAL**, est destinée au dépôt et à la diffusion de documents scientifiques de niveau recherche, publiés ou non, émanant des établissements d'enseignement et de recherche français ou étrangers, des laboratoires publics ou privés.

Membrane proteocomplexome of *Campylobacter jejuni* using 2-D blue native/SDS-PAGE combined to bioinformatics analysis

Odile Tresse^{1*}, Alizée Guérin¹, Sheiam Sulaeman¹, Laurent COQUET^{2, 3}, Armelle Menard⁴, Frederique Barloy-Hubler⁵, Emmanuelle Dé^{2, 3}

¹INRA Centre Angers-Nantes Pays de la Loire, France, ²UMR CNRS 6270 Polymères de laboratoire Biopolymères Surfaces (PBS), France, ³Plateforme protéomique PISSARO IRIB - ROUEN, France, ⁴INSERM U1053 Bordeaux Recherche en Oncologie Translationnelle, France, ⁵UMR6290 Institut de Genetique et Developpement de Rennes (IGDR), France

Submitted to Journal:
Frontiers in Microbiology

Specialty Section:
Food Microbiology

Article type:
Original Research Article

Manuscript ID:
530906

Received on:
30 Jan 2020

Revised on:
12 Oct 2020

Accepted on:
14 Oct 2020

Frontiers website link:
www.frontiersin.org

Conflict of interest statement

The authors declare that the research was conducted in the absence of any commercial or financial relationships that could be construed as a potential conflict of interest

Author contribution statement

OT conceived the work; SS, LC and AG performed the experiments; AG prepared the manuscript and the figures, OT finished the writing and the figures, OT, ED, LC, FBH and AM revised the manuscript.

Keywords

Foodborne pathogen, proteomics, Functional Genomics, complexes, Membrane Proteins, efflux pumps, regulation, Blue native electrophoresis

Abstract

Word count: 260

Campylobacter is the leading cause of human bacterial foodborne infections in developed countries. The perception cues from biotic or abiotic environments by the bacteria are often related to bacterial surface and membrane proteins that mediate the cellular response for the adaptation of *Campylobacter jejuni* to the environment. These proteins function rarely as a unique entity, they are often organized in functional complexes. In *C. jejuni*, these complexes are not fully identified and some of them remain unknown. To identify putative functional multi-subunit entities at the membrane subproteome level of *C. jejuni*, a holistic non a priori method was addressed using two-dimensional blue native /Sodium dodecyl sulfate (SDS) polyacrylamide gel electrophoresis (PAGE) in strain *C. jejuni* 81-176. Couples of acrylamide gradient/migration-time, membrane detergent concentration and hand-made strips were optimized to obtain reproducible extraction and separation of intact membrane protein complexes (MCPs). MCPs were subsequently denatured using SDS-PAGE and each spot from each MCP was identified by mass spectrometry. Altogether, 21 MCPs could be detected including multihomooligomeric and multiheterooligomeric complexes distributed in both inner and outer membranes. Function, conservation and regulation of MCPs across *C. jejuni* strains were inspected by functional and genomic comparison analyses. In this study, relatedness between subunits of two efflux pumps, CmeABC and MacABputC was observed. In addition, a consensus sequence CosR-binding box in promoter regions of MacABputC was identified in *C. jejuni* but not in *C. coli*. The MCPs identified in *C. jejuni* 81-176 membrane are involved in protein folding, molecules trafficking, oxidative phosphorylation, membrane structuration, peptidoglycan biosynthesis, motility and chemotaxis, stress signaling, efflux pumps and virulence.

Contribution to the field

On behalf of the authors, I would like to submit our manuscript entitled " Membrane proteocomplexome of *Campylobacter jejuni* using 2-D blue native/SDS-PAGE combined to bioinformatics analysis" to Frontiers in Microbiology in your research topic. The perception cues from biotic or abiotic environments by the bacteria are often related to bacterial surface and membrane proteins that mediate the cellular response for the adaptation of to the environment. As *Campylobacter jejuni* is the leading cause of human bacterial foodborne infections and its adaptation mechanisms remains to be elucidated, we aimed at exploring protein machineries of *C. jejuni* at the membrane level using proteocomplexomic approach. This work results of a fruitful collaboration between experts on proteomics in *Campylobacter* (Dr Odile Tresse), LC MS/MS protein identification through PISSARO proteomic platform (Dr Emmanuelle Dé and Dr Laurent Coquet), bioinformatics (Dr Barbloy-Hubler) and protein complexomics (Armelle Ménard). Results indicated the presence of multihomooligomeric and multiheterooligomeric complexes distributed in both inner and outer membranes of *C. jejuni*. Function, conservation and regulation of complexes across *C. jejuni* strains were inspected by functional and genomic comparison analyses. Relatedness between subunits of two efflux pumps, CmeABC and MacABputC was observed. A consensus sequence CosR-binding box in promoter regions of MacABputC was also identified in *C. jejuni* but not in *C. coli*. Altogether, this work contributes to better understand proteins machineries and their regulations in *C. jejuni* membrane. All co-authors are in agreement with the content of the manuscript and there is neither financial interest nor conflict of interest to report. We certify that this submission corresponds to an original work that it is not under review in any other journals. Dr Odile Tresse, CR-HAB INRAE

Funding statement

Alizée Guérin was financed by INRAE through the program RFI "Food for Tomorrow in region Pays de la Loire and this study was supported by CompCamp project.

Ethics statements

Studies involving animal subjects

Generated Statement: No animal studies are presented in this manuscript.

Studies involving human subjects

Generated Statement: No human studies are presented in this manuscript.

Inclusion of identifiable human data

Generated Statement: No potentially identifiable human images or data is presented in this study.

Data availability statement

Generated Statement: No datasets were generated or analyzed for this study.

In review

1 Membrane proteocomplexome of *Campylobacter jejuni* using 2-D blue native/SDS-PAGE
2 combined to bioinformatics analysis

3
4
5 Alizée Guérin¹, Sheiam Sulaeman¹, Laurent Coquet^{2,3}, Armelle Ménard⁴, Frédérique Barloy-
6 Hubler⁵, Emmanuelle Dé² and Odile Tresse^{1*}

7
8
9 ¹INRAE, 44316 Nantes, France

10 ²Normandie Université, UNIROUEN, INSA Rouen, CNRS, UMR6270 Laboratoire Polymères
11 Biopolymères Surfaces, 76000 Rouen, France,

12 ³Normandie Université, UNIROUEN, plateforme PISSARO, IRIB, Mont-Saint-Aignan, France

13 ⁴Univ. Bordeaux, INSERM, UMR1053 Bordeaux Research in Translational Oncology,
14 BaRITOn, 33076 Bordeaux, France

15 ⁵ Univ. Rennes, CNRS, IGDR (Institut de génétique et développement de Rennes) - UMR 6290,
16 F35000 Rennes, France

17
18
19
20
21
22
23
24
25
26
27 *Corresponding author. Mailing address: ¹INRAE, CS71627, 44316 Nantes, France. Phone:
28 +33 (0)240 675 006 Email: odile.tresse@inrae.fr

31 **Abstract**

32

33 *Campylobacter* is the leading cause of the human bacterial foodborne infections in the
34 developed countries. The perception cues from biotic or abiotic environments by the bacteria
35 are often related to bacterial surface and membrane proteins that mediate the cellular response
36 for the adaptation of *Campylobacter jejuni* to the environment. These proteins function rarely
37 as a unique entity, they are often organized in functional complexes. In *C. jejuni*, these
38 complexes are not fully identified and some of them remain unknown. To identify putative
39 functional multi-subunit entities at the membrane subproteome level of *C. jejuni*, a holistic
40 non *a priori* method was addressed using two-dimensional blue native/Sodium dodecyl
41 sulfate (SDS) polyacrylamide gel electrophoresis (PAGE) in strain *C. jejuni* 81-176. Couples
42 of acrylamide gradient/migration-time, membrane detergent concentration and hand-made
43 strips were optimized to obtain reproducible extraction and separation of intact membrane
44 protein complexes (MCPs). The MCPs were subsequently denatured using SDS-PAGE and
45 each spot from each MCP was identified by mass spectrometry. Altogether, 21 MPCs could
46 be detected including multihomooligomeric and multiheterooligomeric complexes distributed
47 in both inner and outer membranes. The function, the conservation and the regulation of the
48 MPCs across *C. jejuni* strains were inspected by functional and genomic comparison analyses.
49 In this study, relatedness between subunits of two efflux pumps, CmeABC and MacABputC
50 was observed. In addition, a consensus sequence CosR-binding box in promoter regions of
51 MacABputC was present in *C. jejuni* but not in *C. coli*. The MPCs identified in *C. jejuni* 81-
52 176 membrane are involved in protein folding, molecule trafficking, oxidative
53 phosphorylation, membrane structuration, peptidoglycan biosynthesis, motility and
54 chemotaxis, stress signaling, efflux pumps and virulence.

55

56 Keywords

57 Foodborne pathogen, proteomics ; functional genomics ; complexes ; blue native
58 electrophoresis; membrane proteins; efflux pumps ; regulation

In review

59 1. Introduction

60 *Campylobacter* is a Gram-negative spiral-shaped bacterium. It has emerged as the leading
61 cause of foodborne bacterial gastroenteritis in humans (Epps et al., 2013;Kaakoush et al.,
62 2015;EFSA and ECDC, 2018). The number of campylobacteriosis cases has been increasing
63 in Europe since 2005 and has reached an incidence of 65 per 100 000 people with 246 158
64 confirmed cases in 2018 (EFSA and ECDC, 2018). Most cases were attributed to *C. jejuni*, an
65 invasive microorganism causing gastroenteritis associated with fever and frequent watery
66 bloody diarrhoea, abdominal pains and occasionally nausea (Moore et al., 2005;Silva et al.,
67 2011;Epps et al., 2013). It is also associated with post-infection complications including the
68 immune-mediated neurological disease Guillain-Barré Syndrome (Nachamkin,
69 2002;Alshekhlee et al., 2008), its variant Miller Fisher Syndrome (Ang et al., 2001) or
70 reactive arthritis (Altekruse et al., 1999). Notably, the infectious dose is considered to be
71 lower than the one for other foodborne pathogens as only 500-800 bacteria trigger human
72 infection (Robinson, 1981;Black et al., 1988;Boyanova et al., 2004;Castano-Rodriguez et al.,
73 2015). *Campylobacter* cost of illness was estimated at 2.4 billion euros per year in Europe
74 (EFSA, 2016). *C. jejuni* infections are mainly associated with consumption of poultry and
75 cross-contamination from poultry products (Hue et al., 2010;Guyard-Nicodeme et al.,
76 2013;Hald et al., 2016). For the first time, the European Commission regulation has amended
77 the regulation (EC) No 2073/2005 in 2017 on the hygiene of foodstuffs as regards
78 *Campylobacter* on broiler carcasses stating a limit of 1000 CFU/g applied from January 2018.
79 This microaerophilic, capnophilic and thermophilic microorganism requires fastidious growth
80 conditions and its growth is rapidly hampered by several environmental stress conditions.
81 Optimal growth is obtained using a modified atmosphere limited in dioxygen and enriched in
82 carbon dioxide, a temperature between 37 °C to 45 °C and a pH between 6.5 and 7.5 (Mace et
83 al., 2015). Nonetheless, *C. jejuni* is able to survive harmful conditions by developing

84 adaptation mechanisms in response to stress conditions throughout the food chain (Atack and
85 Kelly, 2009; Rodrigues et al., 2016). Living as biofilms is also a phenotypical feature that was
86 demonstrated for *C. jejuni*, indicating multiple surviving ways outside hosts (Turonova et al.,
87 2015).

88 Proteomic techniques have been applied to *Campylobacter* to better understand how changes
89 in genetic expression, bacterial state, nutrient limitation, food plant processing and
90 environmental conditions could affect *C. jejuni* at the protein level (Tresse, 2017). Natural
91 compartmentalization has facilitated subfraction proteome analyses of *Campylobacter* such as
92 the cytosolic proteome (Kalmokoff et al., 2006; Bieche et al., 2012; Asakura et al., 2016), the
93 membrane proteome (Seal et al., 2007; Cordwell et al., 2008; Scott et al., 2014; Watson et al.,
94 2014), the inner or outer membrane proteome (Sulaeman et al., 2012) and the exoproteome
95 (Kaakoush et al., 2010). In addition, the genomic and computational era have brought exciting
96 and challenging prospects for proteomics like assigning a function to each protein and
97 subsequently its relationship to other proteins in the cell. Functional genomics and protein
98 structural modelling approaches can predict protein-protein interactions (PPIs), which
99 constitutes the theoretical protein interactome of an organism. Predicted interactomes,
100 including potential stable or transient PPIs, are limited to databases content but PPIs already
101 demonstrated to be biologically functional, specific genetic organizations (operons, gene
102 clusters and regulons) or structural features (domains and loops) (Planas-Iglesias et al.,
103 2013; Wetie et al., 2013). Genomic analyses of the main pathogenic species of
104 *Campylobacter*, revealed a lack of some of the well-described organizations into operons or
105 gene clusters in Gram-negative bacteria (Parkhill et al., 2000). For instance, genes involved in
106 the amino-acid biosynthesis are scattered in distinct loci across the genome of *C. jejuni*
107 whereas they are organised into operons in other bacteria. In *H. pylori*, the closest specie
108 relative to *Campylobacter*, the presence of some genetic elements organized into operons,

109 gene clusters or islands could have contributed to the specialization of this pathogen (Sohn
110 and Lee, 2011; You et al., 2012). In *C. jejuni*, the virulence variation among strains could not
111 be assigned to any specific genetic organization other than point mutations in the virulence-
112 associated genes or indels in individual loci (Bell et al., 2013). A reduced genetic organization
113 has probably participated to the idiosyncrasy of *C. jejuni*.

114 The alternative method to identify PPIs, which does not result necessary from a
115 specific genetic organization, is to detect complexes of proteins using non-hypothesis driven
116 methods. When these complexes are composed of only protein subunits, the global approach
117 is called proteocomplexomic. This is the case of the two-dimensional (2-D) blue native
118 (BN)/SDS-PAGE which aims at highlighting intact protein complexes using mild non-ionic
119 and non-denaturing detergents (Dresler et al., 2011; Lasserre and Menard, 2012; Wohlbrand et
120 al., 2016). This method consists in separating native protein complexes according to their
121 molecular mass during the first dimension and subsequently in separating protein subunits of
122 each complex in SDS-denaturated conditions in an orthogonal second dimension. It has been
123 applied with success to monitor oligomeric state, stoichiometry and protein subunit
124 composition of protein complexes.

125 This study aimed at exploring protein machineries of *C. jejuni* at the membrane level.
126 The bacterial membrane as a hydrophobic lipid structure is a suitable site for protein complex
127 organization. Numerous well-characterized proteins embedded in the membrane are organized
128 into functional units involved in various cellular processes. These membrane protein
129 complexes (MPCs) could be also influenced by the membrane structural integrity and their
130 molecular environment (Sachs and Engelman, 2006). In *didermata* such as *C. jejuni*, MPCs
131 could be either organized throughout both membranes and the periplasmic space or
132 specifically in the inner or in the outer membrane. The first objective was to apply and to
133 optimize 2-D BN/SDS-PAGE technique on the *C. jejuni* membrane proteins to obtain

134 reproducible gels. The second goal was to identify MPCs present in *C. jejuni* during optimal
135 growth. As this analysis was conducted on the membrane compartment it was called
136 membrane proteocomplexomic analysis.

137

138 2. Material and methods

139 2.1. 1. Bacterial cell cultures and sample preparation

140 The virulent *C. jejuni* strain 81-176 (NC_008787), whose whole genome is available in
141 Genoscope Platform (MicroScope Vallenet et al., 2017), was selected for the experiments. A
142 loopful of frozen 81-176 cells culture, conserved at -80 °C in Brain-Heart Infusion (BHI)
143 broth (Biokar, Beauvais, France) containing 20% sterile glycerol, was cultured on fresh
144 Karmali agar plates (Oxoid, Dardilly, France) (Air Liquid, Paris, France) at 42 °C for 48 h in
145 microaerobic conditions (MAC) generated using gas replacement jars operated by MACSmics
146 gassing system (BioMérieux, France) with a gas blend composed of 5% O₂, 10% CO₂ and
147 85% N₂ (Air Liquid, Paris, France) and 4 filled/flushed cycles at -50 kPa as described in
148 Mace *et al.*, 2015 (Mace et al., 2015). Cultures were obtained by inoculating
149 500 mL of BHI broth in a 1-L flask and incubating them for 16 h under MAC at 42 °C in a
150 rotary shaker.

151 2.2. Membrane protein complex (MPC) extraction

152 The cells were harvested by centrifugation for 20 min at 4 °C at 6 000 g. The supernatant was
153 discarded and about 3 g of dry pellet was obtained. The cells were washed twice with lysis
154 buffer containing 50 mM Tris, 750 mM 6-amino-n-caproic acid as a zwitterionic salt, with
155 each wash followed by centrifugation at 6 000 g for 20 min at 4 °C. The cells were then
156 resuspended in 5.5 mL of lysis buffer supplemented with 60 µL phenylmethylsulfonyl
157 fluoride (PMSF) and sonicated at 50 kHz for 6 x 30 s with 5 min intervals on ice (Vibracell
158 72434, Bioblock Scientific, Illkirch, France) as previously described by Bieche *et al.* (Bieche

159 et al., 2012). The proteins present in the supernatant were then collected and centrifuged twice
160 at 10 000 *g* for 30 min at 4 °C in order to remove the cellular debris. The whole protein lysate
161 was treated with 0.2 mg/ml DNaseI for 1 h at 25 °C and then ultracentrifuged at 100 000 *g* for
162 1 h at 4 °C. The pellet containing membrane complexes was resuspended in 10 mL of lysis
163 buffer with 50 µL PMSF supplemented with the mild detergent Dodecyl-β-D-Maltoside
164 (DDM) (Sigma, France) at concentrations ranging from 1 to 5% (w/v) to maintain the
165 integrity of protein complexes and limiting dissociation or denaturation as previously
166 recommended by Bernarde *et al.* (Bernarde et al., 2010b). After 15 min on ice, each sample
167 solubilized with DDM was directly ultra-centrifuged at 100 000 *g* for 1 h at 4 °C. The MPC
168 extraction was performed in triplicate from three independent cultures. Aliquots of the
169 supernatant containing the membrane protein complexes were stored at -80 °C. The protein
170 concentration of membrane complexes was determined using the Micro BCA™ Protein Assay
171 Kit (Perbio Science, Brebieres, France) according to the manufacturer protocol.

172 2.3. MPC separation using 2-D BN/SDS-PAGE

173 2.3.1. First dimension in native conditions (BN-PAGE)

174 The first dimension was performed in a blue native polyacrylamide gel (BN-PAGE)
175 according to Schagger (Schagger and von Jagow, 1991) with the following modifications. The
176 MCP separation using BN-PAGE gels (15 cm x 16 cm x 0.1 cm) was assayed on linear
177 acrylamide gradients: 4-14% (w/v), 4-18% (w/v), 8-18% (w/v) or 10-20% (w/v) using a
178 gradient forming unit and Protean II cell (Biorad, Hercules, CA, USA). Each separating gel
179 was overlaid with a 3% stacking BN-PAGE. Both anode and cathode buffers contained
180 50 mM Tris and 75 mM Glycine. Only the cathode buffer was supplemented with 0.002%
181 (w/v) Coomassie Blue G250 (Serva Biochemicals, Heidelberg, Germany). The assembly of
182 gels were embedded with anode and cathode buffers and maintained at 4 °C for 3 h before
183 loading the protein sample. A volume of 1-5 µL of sample buffer (500 mM 6-amino-*n*-caproic

184 acid and 5% Serva blue G) was added to DDM-solubilized membrane protein complex
185 samples. Thyroglobulin (669 kDa), ferritin (440 kDa), catalase (232 kDa), lactate
186 dehydrogenase (140 kDa) and BSA (67 kDa) were used as high molecular weight native
187 protein marker mixture (GE Healthcare, Buckinghamshire, UK). The migration was run at
188 4 °C with 1 W per gel and limited at 150 V and 90 mA during 4 h to 48 h according to the
189 assays.

190 To check the optimal solubilisation of the protein complexes using DDM, migration through
191 BN-PAGE was performed as described above with 3% stacking gel. Samples of 10 or 20 µg
192 of protein complexes solubilized in 1, 2 or 5% (w/v) DDM were prepared as described above
193 and loaded for each lane of the BN-PAGE. For protein complex analyses, gels were silver
194 stained and scanned with a GS-800 densitometer (Bio-Rad) operated with the QuantityOne®
195 software (Bio-Rad) at the resolution of 42.3 microns as described previously by
196 Sulaeman *et al.* (Sulaeman *et al.*, 2012). For the protein identification, the gels were loaded
197 with 50 µg of protein complexes. Following the 1-D migration, the protein complexes in the
198 BN-PAGE were fixed using the kit Bio Safe™ Coomassie G-250 Stain (Biorad) according to
199 the manufacturer's instructions.

200 2.3.2. Second-dimension SDS-PAGE

201 The second dimension was performed under denaturing conditions using 10% (w/v)
202 acrylamide SDS-PAGE (15 cm x 16 cm x 0.15 cm). An individual lane was cut off from the
203 first dimension BN-PAGE using a glass plate. Gel lane was equilibrated for 5 min in a buffer
204 containing 1% (w/v) SDS and 125 mM Tris. Then, the proteins were reduced for 15 min into
205 equilibrating buffer supplemented with 50 mM dithiothreitol (DTT) (Sigma, France), and
206 subsequently alkylated for 15 min in equilibrating buffer supplemented with 125 mM
207 iodoacetamide (Biorad). An ultimate washing step lasting 5 min was performed in the

208 equilibrating buffer without supplement. After polymerization of the separating SDS-PAGE
209 and equilibration, the gel lane was laid on a plastic support and introduced between the gel
210 glass plates over the separation gel and embedded with low-melting agarose. Migration was
211 carried out for 4 h at 16 °C at 300 V maximum and 10 mA/gel for the first 45 min and then at
212 20 mA/gel. After migration, proteins were silver stained and scanned as described above.

213 2.4. In-gel trypsin digestion

214 The silver-stained spots separated by SDS-PAGE were excised manually. At first, the spots
215 were discoloured, then washed and reduced/alkylated using an automated system (MultiProbe
216 II, Perkin Elmer, France) as following: each spot was washed several times in water, once in
217 25 mM ammonium carbonate and dehydrated with acetonitrile (ACN). After drying the gel
218 pieces, the reduction was achieved by incubation for 1 h with 10 mM DTT at 55 °C. The
219 alkylation was achieved by incubation the samples with 25 mM iodoacetamide for 1 h at room
220 temperature. Finally, the gel spots were washed three times in water for 10 min, again
221 alternating between ammonium carbonate and ACN. The gel pieces were completely dried
222 before trypsin digestion and rehydrated by trypsin addition. The digestion was carried out
223 overnight at 37 °C. The gel fragments were subsequently incubated twice for 15 min in a
224 H₂O/ACN solution and in ACN to allow extraction of peptides from the gel pieces. The
225 peptide extracts were then pooled, dried and dissolved in 10 µL starting buffer for
226 chromatographic elution, consisting of 3% (v/v) ACN and 0.1% (v/v) formic acid in water.

227 2.5. Protein identification by LC MS/MS

228 The peptides were enriched and separated using a lab-on-a-chip technology (Agilent, Massy,
229 France) and fragmented using an on-line XCT mass spectrometer (Agilent). The
230 fragmentation data were interpreted using the Data Analysis program (version 3.4, Bruker
231 Daltonic, Billerica, MA, USA). For the protein identification, the MS/MS peak lists were

232 extracted, converted into mgf-format files and compared to the *C. jejuni*, strain 81-176 protein
233 database (UniprotKB, CP000538 for the chromosome, CP000549 for plasmid pTet and
234 CP000550 for plasmid pVir) with the MASCOT Daemon search engine (version 2.6.0; Matrix
235 Science, London, UK). The following search parameters were used: trypsin was used as the
236 cutting enzyme, the mass tolerance for monoisotopic peptide window was set to ± 1.0 Da and
237 the MS/MS tolerance window was set to ± 0.5 Da. Two missed cleavages were allowed.
238 Carbamidomethylation, oxidized methionine, acetylation and pyroglutamate in Nt and
239 amidation in Ct were chosen as variable modifications. Generally, the peptides with
240 individual ions scores higher than the score indicated for $p < 0.05$ were selected. The proteins
241 with two or more unique peptides matching the protein sequence were automatically
242 considered as a positive identification. The main raw data are presented in Table S1. Other
243 raw data are available upon request.

244

245 2.6. Western blotting

246 The western blots of 2-D BN/SDS PAGE were performed according to Sulaeman *et al.*,
247 (2012) (Sulaeman et al., 2012). Briefly, prior to transfer, the 2-D SDS gels were cut into two
248 horizontal sections and each section was soaked for 15 min in transfer buffer. Then, the
249 proteins of each gel section were transferred to a nitrocellulose membrane by electrophoresis
250 using Mini Trans Blot (Bio-Rad). The transferred proteins were then probed with a 1/2000
251 dilution of antibody anti-PorA or antibody anti-CadF. The immunoreactive proteins were
252 detected using a 1/2000 dilution goat-anti-rabbit alkaline phosphatase antibody (Anti-Rabbit
253 IgG, F(avb)2 fragment-Alkaline Phosphatase, Sigma, Saint Quentin Fallavier, France),
254 followed by BCIP/NBT staining (Biorad). Gels were scanned using the GS-800 Imaging
255 densitometer (BioRad).

256 2.7. Bioinformatic analyses

257 2.7.1. *In silico* determination of complex function

258 The presence and organization of genes encoded protein subunits of identified complexes in
259 81-176 and other *Campylobacter* complete genomes was explored using the Platform
260 MicroScope described in Vallenet et al., 2017. The biological function of these proteins and
261 complexes were inferred using KEGG and Microcyc (Kanehisa et al., 2016). The
262 conformation analyses of the proteins alone or in a complex were performed using UniProt
263 (Zommiti et al., 2016), RCSB (Stephen et al., 2018), RCSB PDB (Young et al., 2018), Swiss-
264 model (Biasini et al., 2014) and OPM (Lomize et al., 2012). The functional links between
265 partners of complex was explored using STRING (Szklarczyk et al., 2017). If the complex
266 protein subunits were not identified in *Campylobacter*, homologous genes were searched
267 using conventional gene alignment tools (BlatN).

268 2.7.2 Phylogenetic tree of efflux pumps

269 The protein sequences of CmeA, CmeB, CmeC and MacA, MacB, putMacC (for putative
270 MacC) on fourteen complete genomes of *C. jejuni* strains and six complete genomes of *C. coli*
271 strains were recovered (Table S1). MAFFT alignments (reference PMID:23329690) and Fast
272 Tree (reference PMID:19377059) phylogenetic trees were performed using Geneious R9 and
273 visualised using FigTree V1.4.3 software (<http://tree.bio.ed.ac.uk/software/figtree/>). The
274 proteins structures predictions were determined using Philius transmembrane prediction server
275 (reference, PMID:18989393) (www.yeastrc.org/philius/pages/philius/runPhilius.jsp).

276 2.7.3 Distribution of efflux pumps CmeABC and MacABputC in bacteria

277 BlastP analyses were performed for each protein sequence of the components of these efflux
278 pumps in *C. jejuni* 81-176 against domain bacteria in RefSeq (NCBI Reference Sequence
279 Database) protein database. The general parameters applied for similarity validation were

280 Max target sequences at 20000, automatically adjust parameters for short input sequences,
281 expect threshold at 10, word size at 6 and max matches in a query range at 0. Scoring
282 parameters were obtained from the blosum62 matrix, gap costs with existence at 11 and
283 extension at one with a conditional compositional score matrix adjustment.

284 2.7.4 Identification of CosR DNA-Binding Box

285 The sequence logo of CosR-binding box previously defined by Turonova *et al.* (Turonova et
286 al., 2017) was used to check the presence of cosR-binding box in the promoter regions of the
287 operons encoding the efflux pumps *cmeABC* and *macABputC* among the complete genomes
288 of *C. jejuni* and *C. coli* (Table S1). For that, a sequence length of maximum 120 pb in the
289 intergenic regions upstream to *cmeA* and *macA* was recovered. Based on these sequences, a
290 new sequence logo of CosR DNA-binding box with sequences was drawn using WebLogo
291 platform (<http://weblogo.threeplusone.com> (Crooks et al., 2004)).

292

293 3. Results

294 3.1. Optimization of protein complex solubilization and separation

295 The BN-PAGE was applied first to check the solubilization efficiency of the extracted MPCs.
296 In order to approach a useful detergent concentration for protein complex solubilization for
297 BN-PAGE, Dodecyl- β -D-Maltoside (DDM) has turned out to be suitable (Schägger, 2002).
298 The solubilisation of the membrane was tested in a concentration of 1, 2 or 5% of DDM. The
299 loading quantities of 10 μ g or 20 μ g of MPCs on BN-PAGE were found appropriate to
300 determine the reliable concentration of DDM detergent for *C. jejuni* (Fig. 1). In native
301 conditions, MPCs migrate according to their mass and their form in space (steric hindrance).
302 The bands detected in BN-PAGE in the range of 20 kDa to 670 kDa indicate that MCPs were
303 **stable** after membrane solubilization and during the separation. All tested concentrations of

304 DDM (1, 2 and 5%) seem to be suitable to solubilize MPCs from *C. jejuni*. However, over the
305 three independent extractions, less reproducibility was obtained with 5% DDM for the lower
306 molecular mass complexes (not shown). Consequently, only 2% DDM were selected to
307 explore MPCs of *C. jejuni* 81-176. In addition, the better separation of MPCs was obtained by
308 extending the migration time **until** 40 h (Fig. S1). Acrylamide gradients of BN-PAGE were
309 also optimized by testing different couples of lower concentrations (ranging from 4% to 10%)
310 and higher concentration (ranging from 14% to 20%). Even though some protein complexes
311 were more distinct on some gradients, the linear gradient which gives more detectable
312 complexes was 4% to 18% of acrylamide. In general, a lack of reproducibility of the 2-D gels
313 and vertical smearing altering the resolution of MPCs subunits on SDS-PAGE were
314 frequently reported. To circumvent these biases, many gels were run in previous studies until
315 obtaining at least three similar replicates. In the present study, obtaining gel repeatability in a
316 consecutive manner was the first goal. This goal was reached by decreasing vertical smearing,
317 adjusting the thickness of the gels, fixing the supports and isolating the homemade strip from
318 glass using **a five-step protocol** (Fig. S1). All these optimization steps resulted in performing
319 consecutive reproducible gels. **The reproducibility was validated once three consecutive**
320 **profiles could be aligned with the same number of detected spots.** The results of optimisation
321 steps during the first and second dimensions are presented in figure S2.

322 3.2. Analysis of 2D-BN/SDS-PAGE data

323 Using the criteria mentioned by Reisinger and Eichacker (Reisinger and Eichacker, 2006), all
324 protein spots that are located vertically below each other with a similar shape on the 2-D were
325 considered as subunits of one MPC. Consequently, the complexes were numbered from the
326 left side to the right side of the 2-D gel and the detected subunits for each complex with a
327 second number starting from the top of the gel (Fig. 2). The spots, which were located side by
328 side in a horizontal row, could potentially be an identical subunit in protein complexes of

329 different molecular masses. If we assume that the molecular mass of a protein complex is
330 increased during assembly of its structural subunits, the analysis of the protein pattern allows
331 to determine the stepwise subunit assembly. The lower towards the higher molecular mass
332 should correspond to complexes located from the right side of the gel towards its left side
333 (Reisinger and Eichacker, 2008). When a complex was composed of subunits from the same
334 gene product, they were called multihomooligomeric complexes and when they were
335 composed of different subunits, they were named multiheterooligomeric complexes as
336 described before (Bernarde et al., 2010b). Some complexes could not be detected due to a
337 relatively low abundance in the membrane, solubilisation parameters or separation
338 parameters. In addition, depending on the solubilisation and separation parameters more than
339 one protein complex could run at the same molecular mass during BN-PAGE. This was
340 observed more frequently for smaller protein complexes. In this case, the spot identification
341 helps to separate different complexes when the biological function was previously described.
342 The solubilisation, the migration parameters, the interaction between subunits and the subunit
343 organization in or associated with the membrane could also result in partial identification of
344 complexes.

345 The identification of the spots was achieved by nanoLC MS/MS and validated using Mascot
346 score (Table 1, Table S1). The western blots using polyclonal antibodies anti-PorA and anti-
347 CadF were used to target specific outer membrane proteins (Fig. S3). Three spots of PorA and
348 one spot of CadF could be identified using Western-blot confirming the identification
349 performed by LC MS/MS. In addition, the LC MS/MS identified two supplementary spots of
350 PorA indicating that it has a probable higher sensitivity than Western-blot according to the
351 protein abundance. As expected, PorA, also named major outer membrane protein (MOMP) is
352 among the predominant proteins. It was previously reported that PorA could account for 45%
353 of the total visible membrane proteins of *C. jejuni* (Cordwell et al., 2008).

354 3.3. Protein complex identification by Two-dimensional (2-D) blue native (BN)/SDS-
355 PAGE

356 Overall, 55 spots were submitted to LC-MS/MS analysis (Fig. 2 and Table 1). Among them,
357 nine isolated spots and all spots of complex 7 could not be identified, although attempts using
358 different MS technologies were performed. No contamination with exogenous protein, like
359 keratin, was detected. The spectrograms seem to show noise-to-signal trouble shootings. Two
360 proteins identified with a low scoring (Mascot score < 30) were discarded from the analysis.
361 The remaining spots could be grouped into 20 complexes according to their location in the
362 gel, identification and biological functions when available. Overall, 39 proteins predicted as
363 membrane proteins or membrane associated proteins were identified indicating the efficiency
364 of the extraction of the protein complexes from *C. jejuni* 81-176. These complexes were
365 grouped according to biological functions of KEGG classification (Table 1). Four complexes
366 are involved in oxidative phosphorylation, two in the respiration process, seven in molecules
367 trafficking, three in protein biosynthesis and folding, one in motility and three with unknown
368 functions in the membrane. Altogether, 6 multiheterooligomeric and fourteen
369 multihomooligomeric complexes were detected (Table 1). Certain identified complexes were
370 already described in *C. jejuni* such as efflux pump CmeABC (Gibreel et al., 2007) validating
371 this technique to identify MPC in this bacteria. However, novel complexes are presented, such
372 as complexes 2 and 8 comprised of FrdABC and FdhAB, respectively. These complexes were
373 already described in *Helicobacter pylori* Bernarde *et al.* (Bernarde et al., 2010a) and
374 *Eubacterium acidaminophilum* (Graentzdoerffer et al., 2003), respectively.

375 3.4. *In silico* analysis of efflux pumps CmeABC and MacAB

376 Among the 20 identified complexes, subunits belonging to two efflux pumps were detected in
377 complex 6 with CmeA, CmeB and CmeC and complex 20 with MacB (Fig. 2 and Table 1).

378 The subunits of these two pumps were further investigated in this study. CmeABC is a
379 multidrug efflux system in *Campylobacter* working as an RND efflux pump (Lin et al.,
380 2002; Akiba et al., 2006; Grinnage-Pulley and Zhang, 2015). It contributes to the resistance
381 acquisition of *Campylobacter* to various antimicrobials including macrolides and
382 fluoroquinolones (Yan et al., 2006; Gibreel et al., 2007; Jeon and Zhang, 2009). This efflux
383 pump has also an important role in the resistance to bile (Lin et al., 2003). It includes the inner
384 membrane drug transporter CmeB, the periplasmic membrane fusion protein CmeA and the
385 outer membrane channel CmeC. These proteins can be glycosylated at various sites (Scott et
386 al., 2011) which could explain two CmeB proteins identified with a different **molecular**
387 **weight** (Fig. 2). The bioinformatics analysis confirmed the organization in operon of the two
388 efflux pumps amongst both *C. jejuni* and *C. coli*. **For the other efflux pump, the subunit**
389 **MacB, previously identified to be associated with MacA, was detected in the**
390 **multihomooligomeric complex 20 which belongs to the efflux pump specific to macrolides**
391 **(Yum et al., 2009; Bogomolnaya et al., 2013).** (Yum et al., 2009; Bogomolnaya et al., 2013).
392 Using Platform MicroScope, STRING, blastp and blastn, both DNA and protein sequences of
393 these efflux pump partners were analysed across *C. jejuni* and *C. coli*. Genes *cmeA* and *macA*
394 are homologous and *cmeC* is homologous to a gene encoding a putative outer membrane
395 protein (CJJ81176_0637) located downstream to *macB*. This putative outer membrane protein
396 contains the same functional domain TolC as the one described in CmeC suggesting that this
397 putative protein is probably the third partner of MacAB efflux pump. **Further experimental**
398 **assays will be required to validate the biological function of this putative protein for**
399 **macrolide efflux pump operation.** The phylogenetic and functional analyses confirm the
400 similarities between proteins sequences of subunits of these two efflux pumps across
401 *Campylobacter* strains (Fig. 4; Table S1). **CmeA and MacA belong to the HlyD superfamily**
402 **showing a structure composed of the signal peptide and the non-cytoplasmic domain.** The

403 phylogenetic analysis of the putative outer membrane protein CJJ81176_0637 confirmed it
404 similarly to CmeC which likely is the third subunit of the efflux pump MacAB (Fig. 4).
405 Considering this data, this putative outer membrane protein was named putative MacC
406 (putMacC) and the system MacABputC. In contrast to the similarity between sequences and
407 structural functions of CmeC and putMacC in one hand and CmeA and MacA in the other
408 hand, differences observed between CmeB and MacB is probably at the origin of the
409 restriction of MacB to macrolides efflux.

410 3.5. Analysis of the potential regulation of MacABC

411 The efflux pump CmeABC was previously shown to be regulated by CmeR and CosR (Lin et
412 al., 2005; Hwang et al., 2012; Grinnage-Pulley et al., 2016) while no regulation was identified
413 for MacABC. Using the CosR binding box sequence (5'-wdnnhdwnwhwwTTwnhhTTd-3')
414 previously described by Turonova *et al.* (Turonova et al., 2017), *in silico* analysis revealed the
415 presence of a CosR-like DNA-binding box upstream to *macA* in *C. jejuni* 81-176. Screening
416 for the presence of the CosR binding box in the promoter region of *macA* in the complete
417 genomes of *C. jejuni* and *C. coli*, this consensus sequence was found in *C. jejuni* but not in
418 *C. coli*. All the binding box DNA sequences of CosR in the *cmeA* promoter region of both
419 *C. jejuni* and *C. coli* strains and the *macA* promoter region of *C. jejuni* strains were compared
420 so as to propose a consensus sequence logo refined for CosR-binding box (Fig. 5).

421 3.6. Distribution of gene subunit encoding CmeABC and MacABputC across Bacteria 422 domain

423 Analyses of genes encoding proteins belonging to these two efflux pumps using across
424 Bacteria domain Blastp analysis indicates that they are mainly observed in proteobacteria
425 (Fig. 6, Table S1). CmeA, CmeB and CmeC were mainly found in the delta/epsilon
426 proteobacteria groups while MacABputC also highly more represented in beta and gamma

427 proteobacteria. Proteins of MacABputC were also found in the fusobacteriaceae family
428 belonging to the fusobacterial phylum (Fig. 6, Table S1). The presence of this third subunit in
429 outer membrane (putMaC and CmeC) is probably crucial for the functionality of these
430 complexes.

431

432 4. Discussion

433 Beyond the protein mapping at the organism or a biological compartment scale using holistic
434 approaches, identifying functional multi-subunit entities at the proteome level is a real
435 challenge. Many cellular processes are carried out by sophisticated multi-subunit protein
436 machineries, *i.e.* different protein complexes maintained by stable protein interactions. These
437 functional entities could be defined as protein complexes composed of a minimal biologically
438 structure of assembled protein subunits necessary for a specific cellular process (Reisinger
439 and Eichacker, 2007). Membrane proteocomplexome of *C. jejuni* 81-176 cultivated in optimal
440 growth conditions was explored using 2-D BN/SDS PAGE. The prerequisite goal was to
441 obtain reproducible profiles after optimizing and stabilising homemade strips. The objective
442 was reached when three consecutive gels with resolved spots could be performed. Twenty-one
443 MPCs were found with this method in *C. jejuni* 81-176 (Fig. 3). We found incomplete
444 complexes suggesting that subunits were probably lost during MPC extraction or unidentified
445 by LC MS/MS.

446 4.1. Oxidative phosphorylation

447 Oxidative phosphorylation is the metabolic pathway in which bacteria use enzymatic
448 complexes to re-oxidize cofactors and produce ATP. It ensures the electron transfer between
449 electron donors and the final electron acceptor which is oxygen for aerobic and microaerobic
450 bacteria such as *C. jejuni*. The redox reactions are carried out by a series of four protein
451 complexes (I, II, III, IV) located in the inner membrane. Membrane proteocomplexomic

452 profiling revealed the presence of complexes involved in oxidative phosphorylation.

453 Complex 19 corresponds to the NADH ubiquinone oxidoreductase, the first complex of the

454 oxidative phosphorylation chain. This complex catalyzes the transfer of two electrons from

455 NADH to quinone with the translocation of four protons across the inner membrane: $\text{NADH} +$

456 $\text{H}^+ + \text{Q} + 4\text{H}^+_{\text{in}} \rightarrow \text{NAD}^+ + \text{QH}_2 + 4\text{H}^+_{\text{out}}$ (Baranova et al., 2007; Weerakoon and Olson,

457 2008; Efremov and Sazanov, 2011; Baradaran et al., 2013). Genomic analysis revealed

458 fourteen genes *nuo* organized in operon in *C. jejuni* and *C. coli* genomes with a highly

459 conserved synteny. NuoFEGDCBI are involved in the hydrophilic domain of the NADH

460 dehydrogenase complex while NuoAHJKLMN is localized into the membrane (Baradaran et

461 al., 2013). The partners of this complex NuoC, NuoD and NuoG detected from our MPC

462 fingerprintings are predicted to be localized on the basal part of the hydrophilic domain, close

463 to the inner membrane. In *E. coli*, NuoC and NuoD are fused and NuoG is close to them

464 (Baranova et al., 2007; Baradaran et al., 2013). If these subunits are similarly organized in

465 *C. jejuni*, this would indicate that 2% DMM MPC extraction, detection and subunit

466 identification mainly selected this part of NADH dehydrogenase complex. The complex 2

467 corresponds to complex II of the oxidative phosphorylation chain. The fumarate reductase

468 complex is generally composed of FrdA, FrdB and FrdC (Weingarten et al., 2009; Guccione et

469 al., 2010; Jardim-Messeder et al., 2017). All three subunits were detected and identified on all

470 the proteocomplexomic fingerprintings performed in the present study. In *C. jejuni*, this inner

471 membrane system is bifunctional being able to catalyze both succinate oxidation and fumarate

472 reduction (Guccione et al., 2010; Hofreuter, 2014). The succinate oxidation is favored under

473 microaerobic conditions while the fumarate reduction is operated under oxygen-limited

474 conditions. All three genes are close located on the genome of both *C. jejuni* and *C. coli*. FrdA

475 is the fumarate reductase flavoprotein, FrdB is the iron-sulfur subunit and FrdC is the

476 cytochrome B-556 subunit. This fumarate reductase complex FrdABC was also described in

477 *H. pylori* (Pyndiah et al., 2007). A fourth partner, FrdD is described in *E. coli* (Rothery et al.,
478 2005). However, the bioinformatic analyses did not reveal any homologous gene to FrdD in
479 *C. jejuni* and *C. coli* genomes. This would indicate that complex 2 does exist and might be
480 functional in *C. jejuni* and *H. pylori* without FrdD subunit. Any subunit of the ubiquinol-
481 cytochrome c reductase, complex III of the oxidative phosphorylation, was not detected in this
482 study. However, predicted functional partners of this proton pump were detected in *C. jejuni*
483 genome: *petA* encoding the iron sulfur subunit, *petB* encoding the cytochrome b subunit and
484 *petC* encoding the cytochrome c1 subunit which indicates the absence of this complex in
485 optimal growth conditions or DMM limitations to extract all MPCs. Partners, function and
486 pathways of cytochrome c oxidase (complex IV) in *Campylobacter* remain elusive. It is
487 encoded by *ccoNOPQ*. The protein CcoO (Complex 9) was detected in our study. It
488 corresponds to the subunit II of cytochrome c oxidase complex with a high affinity for O₂
489 (Cosseau and Batut, 2004; Hofreuter, 2014). In complex V, the ATP synthase is usually
490 composed of nine subunits, AtpABCDEFFGH often identified as subunit α , A, ϵ , β , C, B, B',
491 γ and δ (Rastogi and Girvin, 1999; Altendorf et al., 2000; Cingolani and Duncan, 2011; Okuno
492 et al., 2011). The bioinformatics analyses revealed that genes *atpF*, *atpF'*, *atpH*, *atpA*, *atpG*,
493 *atpD* and *atpC* are close located in *C. jejuni* and *C. coli* genomes while genes *atpB* and *atpE*
494 are present in different loci. The proteocomplexomic analysis identified AptD (also called
495 subunit β in complex 11). The membrane-bound ATP synthase is a key energy carrier in
496 bacteria using the energy of an electrochemical ion gradient and the synthesis of ATP from
497 ADP with inorganic phosphate (Rastogi and Girvin, 1999; Altendorf et al., 2000; Cingolani
498 and Duncan, 2011; Okuno et al., 2011).

499 4.2 Respiration

500 The complex formate deshydrogenase (complex 8) contributes to the respiration process by
501 producing CO₂ from formate oxidation (Hofreuter, 2014). This complex is composed of two

502 FdhA and FdhB, two subunits detected on complexomic fingerprintings. As an asaccharolytic
503 microorganism, carbon supply in *Campylobacter* is ensured from amino and organic acids and
504 formate is one of the preferred substrate when hosted in poultry. The second detected complex
505 involved the respiration process is hydrogenase complex HydAB complex 12. Two HydB
506 with different weights (around 75 kDa and 130 kDa) were identified in complex 12 indicating
507 the possible presence of a dimeric form of HydB (spot 12.1) in *C. jejuni* membrane. For these
508 two complexes, single conserved copies of the encoding genes were observed in all analyzed
509 genomes except for *C. jejuni* 4031 where a second copy of *FdhA* was found. Two other
510 subunits for each complex (FdhC/FdhD and HydC/HydD) were previously identified in
511 *C. jejuni* (Andresen and Makdessi, 2008;Smart et al., 2009;Weerakoon et al., 2009;Pryjma et
512 al., 2012;Shaw et al., 2012;Hofreuter, 2014). These two other partners interact with the main
513 ones only under environmental stress conditions. The genes encoding these environment
514 dependent conditions are present on *C. jejuni* and *C. coli* genomes. As MPCs of *C. jejuni* 81-
515 176 were explored under optimal growth in our study, it is not a surprise not having detected
516 them.

517 4.3. Biosynthesis and folding of proteins

518 Several proteins are biosynthesized and folded by different complexes localized in membrane.

519 **Different membrane protein complexes were extracted and identified in this study.**

520 The **chaperonin** GroEL (complex 0) is a cylindrical complex with two stacked heptameric
521 rings with ATPase activity that binds non-native substrate protein (SP). GroEL is associated
522 with cofactor GroES and form a nano-cage where SP can be folded up (Klancnik et al.,
523 2006;Chi et al., 2015;Haldar et al., 2015;Motojima and Yoshida, 2015;Hayer-Hartl et al.,
524 2016). As its cofactor GroES has a too small molecular weight (10 kDa), it could not be
525 detected on our profiling fingerprinting. Another complex (complex 4) playing a role in
526 protein folding was detected. DsbB-DsbA is a disulfide bond generation system operating in

527 the oxidative pathway (Inaba et al., 2006;Inaba and Ito, 2008;Ito and Inaba, 2008;Grabowska
528 et al., 2011;Sperling et al., 2013). In this study, only DsbB subunit was identified although
529 two *dsbA* genes with 51% homology were present in *C. jejuni* 81-176 genome. DsbB
530 localized in inner-membrane interacts with the periplasmic dithiol oxidase DsbA (Inaba et al.,
531 2006;Inaba and Ito, 2008).

532 4.4. Molecules trafficking in membrane

533 Several membrane protein complexes identified in this study have a function in molecule
534 trafficking through the *C. jejuni* 81-176 membrane. These complexes play an important role
535 in adaptation and virulence capabilities. For instance, the major *Campylobacter* porin PorA
536 was extracted and identified in the complexes 3 and 13. This porin corresponding to MOMP,
537 involved in the adaptation of *Campylobacter* to host environments (De et al., 2000;Zhang et
538 al., 2000;Clark et al., 2007;Ferrara et al., 2016), is a multihomooligomeric porin with three
539 PorA subunits (Zhang et al., 2000;Ferrara et al., 2016). This porin can be identified in three
540 conformational forms including the folded monomer (35 kDa), the denatured monomer (40 to
541 48 kDa), and the native trimer (120 to 140 kDa) (Huyer et al., 1986;Zhang et al., 2000). In our
542 gel, two complexes corresponding to native trimer MOMP at two different weights were
543 identified. The complex 13 was estimated between 120-140 kDa and after subunit separation
544 proteins corresponding to the folded monomer at 35 kDa and the denatured monomer between
545 40 and 48 kDa could be detected as previously described by Zhang *et al.* 2000 (Zhang et al.,
546 2000). In the complex 3, the spot with apparent **weight** between 350 kDa and 400 kDa could
547 correspond to the fusion of two trimeric MOMPs. The associated forms of MOMP in the
548 complex 3 with likely a folded monomer, denatured monomer and a truncated form at 16 kDa
549 was not previously described.

550 4.5. Antibiotic efflux pumps

551 In this work, units of complexes corresponding to two efflux pumps CmeABC and MacAB
552 were detected (complex 6 and 20). These two efflux pumps were known to play a role in
553 antimicrobials resistance. The multidrug efflux pump CmeABC was more studied compared
554 to the macrolide efflux pump MacABputC in *Campylobacter* (Lin et al., 2002;Lin et al.,
555 2003;Akiba et al., 2006;Yan et al., 2006;Gibreel et al., 2007;Jeon and Zhang, 2009;Grinnage-
556 Pulley and Zhang, 2015). In our study, the genetic and proteomic similarities between the
557 constitutive proteins of these efflux pumps were highlighted by bioinformatics analyses. We
558 were able to identify a potential third partner of the macrolide efflux pump, putMacC with a
559 functional domain TolC similar to CmeC. Subunits composing these two efflux pumps were
560 mainly found in the proteobacteria phylum. Furthermore, the presence of CosR-binding box
561 of the upstream sequences of *macA* was found in *C. jejuni* strains. However, this CosR-
562 binding box could not be detected upstream *macA* in *C. coli* strains. Further biological
563 analyses are required to explore the potential rule of CosR to regulate expression of
564 transcripts of this macrolide efflux pump and to state its presumptive species specificity.

565 4.6. New membrane protein complexes

566 Two complexes (complex 1 and 14) were extracted and their subunits could be identified. The
567 subunits of the complex 1, IlvC a ketol acid reductoisomerase and Ftn a nonheme iron-
568 containing ferritin were detected on the same horizontal line. IlvC is involved in L-isoleucine
569 and L-valine biosynthesis (Pyndiah et al., 2007;Wu et al., 2016) while Ftn has a role in storing
570 available cytosolic iron and to reduce cellular toxicity under conditions of intermittent or
571 constant iron excess during infection (Wai et al., 1996). There are few information concerning
572 these two proteins in *Campylobacter* and no interactions were reported. Complexes 10 and 14
573 are made of two isoforms of the methyl accepting chemotaxis protein CJJ_0180. This protein
574 plays a role in chemotaxis and colonization of the gastrointestinal tract (Gonzalez et al.,
575 1998;Zautner et al., 2012;Li et al., 2014;Chandrashekhar et al., 2015). However, weight of

576 complexes 10 and 14 are different, indicating that these multihomooligomeric complex might
577 be composed of different forms of the subunit as it was described for MOMP complex.

578

579 To conclude, this study is the first 2-D BN/SDS-PAGE method applied to identify membrane
580 proteocomplexome of *Campylobacter jejuni*. Although not all the subunits of functional
581 complexes in the membrane of *C. jejuni* could be detected, functional genomics analyses
582 assisted us in reconstituting probable functional complexes. For instance, we were able to
583 pinpoint a potential third partner in the macrolide efflux pump and raised hypothesis
584 concerning its regulation by CosR. The 2-D BN/SDS-PAGE raised also limitations for
585 studying bacterial proteocomplexomes. Assignment of spots to independent membrane
586 protein complexes in low molecular weight areas is less easy. In certain cases, proteins
587 complexes were probably too weakly expressed as compared to others, or absent in optimal
588 conditions. The tune up of DDM concentration, the conformation of complexes and their
589 location, as full or part of the membrane, might contribute to the extraction of entire and
590 stable complexes. Altogether, this study has allowed to better describe the membrane
591 proteocomplexome of *C. jejuni* providing new focus for further studies of protein complexes
592 previously annotated with unknown functions.

593

594 Acknowledgments

595 The authors are grateful to Pr Mégraud (Univ. Bordeaux, INSERM, UMR1053 Bordeaux
596 Research in Translational Oncology, BaRITOn, 33076 Bordeaux) for helping us to develop
597 complexomic analyses. Thank you to Lucile Bougro for her technical assistance. Alizée
598 Guérin was financed by INRAE through the program RFI “Food for Tomorrow in region Pays
599 de la Loire and this study was supported by CompCamp project. This work was presented in

600 part at the 19th International Workshop on Campylobacter, Helicobacter and Related
601 Organisms: CHRO, 2017.

602

In review

603 Reference

- 604 Akiba, M., Lin, J., Barton, Y.W., and Zhang, Q.J. (2006). Interaction of CmeABC and CmeDEF in
 605 conferring antimicrobial resistance and maintaining cell viability in *Campylobacter jejuni*.
 606 *Journal of Antimicrobial Chemotherapy* 57, 52-60.
- 607 Alsheklee, A., Hussain, Z., Sultan, B., and Katirji, B. (2008). Guillain-Barre syndrome - Incidence and
 608 mortality rates in US hospitals. *Neurology* 70, 1608-1613.
- 609 Altekruze, S.F., Stern, N.J., Fields, P.I., and Swerdlow, D.L. (1999). *Campylobacter jejuni* - An emerging
 610 foodborne pathogen. *Emerging Infectious Diseases* 5, 28-35.
- 611 Altendorf, K., Stalz, W.D., Greie, J.C., and Deckers-Hebestreit, G. (2000). Structure and function of the
 612 F₀ complex of the ATP synthase from *Escherichia coli*. *Journal of Experimental Biology* 203,
 613 19-28.
- 614 Andreesen, J.R., and Makdessi, K. (2008). "Tungsten, the surprisingly positively acting heavy metal
 615 element for prokaryotes," in *Incredible Anaerobes: From Physiology to Genomics to Fuels*,
 616 eds. J. Wiegel, R.J. Maier & M.W.W. Adams. (Oxford: Blackwell Publishing), 215-229.
- 617 Ang, C.W., De Klerk, M.A., Endtz, H.P., Jacobs, B.C., Laman, J.D., Van Der Meche, F.G.A., and Van
 618 Doorn, P.A. (2001). Guillain-Barre syndrome- and Miller Fisher syndrome-associated
 619 *Campylobacter jejuni* lipopolysaccharides induce anti-GM(1) and anti-GQ(1b) antibodies in
 620 rabbits. *Infection and Immunity* 69, 2462-2469.
- 621 Asakura, H., Kawamoto, K., Murakami, S., Tachibana, M., Kurazono, H., Makino, S., Yamamoto, S.,
 622 and Igimi, S. (2016). Ex vivo proteomics of *Campylobacter jejuni* 81-176 reveal that FabG
 623 affects fatty acid composition to alter bacterial growth fitness in the chicken gut. *Research in*
 624 *Microbiology* 167, 63-71.
- 625 Atack, J.M., and Kelly, D.J. (2009). Oxidative stress in *Campylobacter jejuni*: responses, resistance and
 626 regulation. *Future Microbiology* 4, 677-690.
- 627 Baradaran, R., Berrisford, J.M., Minhas, G.S., and Sazanov, L.A. (2013). Crystal structure of the entire
 628 respiratory complex I. *Nature* 494, 443-448.
- 629 Baranova, E.A., Holt, P.J., and Sazanov, L.A. (2007). Projection structure of the membrane domain of
 630 *Escherichia coli* respiratory complex I at 8 angstrom resolution. *Journal of Molecular Biology*
 631 366, 140-154.
- 632 Bell, J., Jerome, J., Plovanch-Jones, A., Smith, E., Gettings, J., Kim, H., Landgraf, J., Lefebure, T.,
 633 Kopper, J., Rathinam, V., St Charles, J., Buffa, B., Brooks, A., Poe, S., Eaton, K., Stanhope, M.,
 634 and Mansfield, L. (2013). Outcome of infection of C57BL/6 IL-10(-/-) mice with
 635 *Campylobacter jejuni* strains is correlated with genome content of open reading frames up-
 636 and down-regulated in vivo. *Microbial Pathogenesis* 54, 1-19.
- 637 Bernarde, C., Lehours, P., Lasserre, J.P., Castroviejo, M., Bonneu, M., Megraud, F., and Menard, A.
 638 (2010a). Complexomics study of two *Helicobacter pylori* strains of two pathological origins:
 639 potential targets for vaccine development and new insight in bacteria metabolism. *Molecular*
 640 *and Cellular Proteomics* 9, 2796-2826.
- 641 Bernarde, C., Lehours, P., Lasserre, J.P., Castroviejo, M., Bonneu, M., Mégraud, F., and Ménard, A.
 642 (2010b). Complexomics study of two *Helicobacter pylori* strains of two pathological origins:
 643 potential targets for vaccine development and new insight in bacteria metabolism. *Molecular*
 644 *& cellular proteomics : MCP* 9, 2796-2826.
- 645 Biasini, M., Bienert, S., Waterhouse, A., Arnold, K., Studer, G., Schmidt, T., Kiefer, F., Gallo Cassarino,
 646 T., Bertoni, M., Bordoli, L., and Schwede, T. (2014). SWISS-MODEL: modelling protein tertiary
 647 and quaternary structure using evolutionary information. *Nucleic Acids Res* 42, W252-258.
- 648 Bieche, C., De Lamballerie, M., Chevret, D., Federighi, M., and Tresse, O. (2012). Dynamic proteome
 649 changes in *Campylobacter jejuni* 81-176 after high pressure shock and subsequent recovery.
 650 *Journal of Proteomics* 75, 1144-1156.
- 651 Black, R.E., Levine, M.M., Clements, M.L., Hughes, T.P., and Blaser, M.J. (1988). Experimental
 652 *Campylobacter jejuni* Infection in Humans. *Journal of Infectious Diseases* 157, 472-479.

653 Bogomolnaya, L.M., Andrews, K.D., Talamantes, M., Maple, A., Ragoza, Y., Vazquez-Torres, A., and
654 Andrews-Polymenis, H. (2013). The ABC-Type Efflux Pump MacAB Protects *Salmonella*
655 *enterica* serovar *Typhimurium* from Oxidative Stress. *Mbio* 4, 11.

656 Boyanova, L., Gergova, G., Spassova, Z., Koumanova, R., Yaneva, P., Mitov, I., Derejian, S., and
657 Krastev, Z. (2004). *Campylobacter* infection in 682 Bulgarian patients with acute enterocolitis,
658 inflammatory bowel disease, and other chronic intestinal diseases. *Diagnostic Microbiology*
659 *and Infectious Disease* 49, 71-74.

660 Castano-Rodriguez, N., Kaakoush, N.O., Lee, W.S., and Mitchell, H.M. (2015). Dual role of
661 *Helicobacter* and *Campylobacter* species in IBD: a systematic review and meta-analysis. *Gut*.
662 Chandrashekhara, K., Gangaiah, D., Pina-Mimbela, R., Kassem, I., Jeon, B.H., and Rajashekhara, G.
663 (2015). Transducer like proteins of *Campylobacter jejuni* 81-176: role in chemotaxis and
664 colonization of the chicken gastrointestinal tract. *Frontiers in Cellular and Infection*
665 *Microbiology* 5, 12.

666 Chi, H.X., Wang, X.Q., Li, J.Q., Ren, H., and Huang, F. (2015). Folding of newly translated membrane
667 protein CCR5 is assisted by the chaperonin GroEL-GroES. *Scientific Reports* 5, 11.

668 Cingolani, G., and Duncan, T.M. (2011). Structure of the ATP synthase catalytic complex (F-1) from
669 *Escherichia coli* in an autoinhibited conformation. *Nature Structural & Molecular Biology* 18,
670 701-U100.

671 Clark, C.G., Beeston, A., Bryden, L., Wang, G.H., Barton, C., Cuff, W., Gilmour, M.W., and Ng, L.K.
672 (2007). Phylogenetic relationships of *Campylobacter jejuni* based on *porA* sequences.
673 *Canadian Journal of Microbiology* 53, 27-38.

674 Cordwell, S.J., Alice, C.L.L., Touma, R.G., Scott, N.E., Falconer, L., Jones, D., Connolly, A., Ben, C., and
675 Djordjevic, S.P. (2008). Identification of membrane-associated proteins from *Campylobacter*
676 *jejuni* strains using complementary proteomics technologies. *Proteomics* 8, 122-139.

677 Cosseau, C., and Batut, J. (2004). Genomics of the *ccoNOQP*-encoded *cbb(3)* oxidase complex in
678 bacteria. *Archives of Microbiology* 181, 89-96.

679 Crooks, G.E., Hon, G., Chandonia, J.M., and Brenner, S.E. (2004). WebLogo: A sequence logo
680 generator. *Genome Research* 14, 1188-1190.

681 De, E., Jullien, M., Labesse, G., Pages, J.M., Molle, G., and Bolla, J.M. (2000). MOMP (major outer
682 membrane protein) of *Campylobacter jejuni*; a versatile pore-forming protein. *FEBS Letters*
683 469, 93-97.

684 Dresler, J., Klimentova, J., and Stulik, J. (2011). Bacterial protein complexes investigation using blue
685 native PAGE. *Microbiological Research* 166, 47-62.

686 Efremov, R.G., and Sazanov, L.A. (2011). Structure of the membrane domain of respiratory complex I.
687 *Nature* 476, 414-U462.

688 Efsa (2016). Scientific report of EFSA and ECDC - The European Union summary report on trends and
689 sources of zoonoses, zoonotic agents and food-borne outbreaks in 2014. *EFSA J.* 13, 4329.

690 Efsa, and Ecdc (2018). European Food Safety Authority, European Centre for Disease Prevention and
691 Control: The European Union Summary Report on Trends and Sources of Zoonoses, Zoonotic
692 Agents and Food-borne Outbreaks in 2017. *EFSA Journal* 2018 16, 5500.

693 Epps, S.V.R., Harvey, R.B., Hume, M.E., Phillips, T.D., Anderson, R.C., and Nisbet, D.J. (2013).
694 Foodborne *Campylobacter*: Infections, Metabolism, Pathogenesis and Reservoirs.
695 *International Journal of Environmental Research and Public Health* 10, 6292-6304.

696 Ferrara, L.G.M., Wallat, G.D., Moynié, L., Dhanasekar, N.N., Aliouane, S., Acosta-Gutiérrez, S., Pagès,
697 J.-M., Bolla, J.-M., Winterhalter, M., Ceccarelli, M., and Naismith, J.H. (2016). MOMP from
698 *Campylobacter jejuni* Is a Trimer of 18-Stranded β -Barrel Monomers with a Ca^{2+} Ion Bound
699 at the Constriction Zone. *Journal of Molecular Biology* 428, 4528-4543.

700 Gibreel, A., Wetsch, N.M., and Taylor, D.E. (2007). Contribution of the CmeABC efflux pump to
701 macrolide and tetracycline resistance in *Campylobacter jejuni*. *Antimicrobial Agents and*
702 *Chemotherapy* 51, 3212-3216.

703 Gonzalez, I., Richardson, P.T., Collins, M.D., and Park, S.F. (1998). Identification of a gene encoding a
704 methyl-accepting chemotaxis-like protein from *Campylobacter coli* and its use in a molecular
705 typing scheme for *campylobacters*. *Journal of Applied Microbiology* 85, 317-326.

706 Grabowska, A.D., Wandel, M.P., Lasica, A.M., Nesteruk, M., Roszczenko, P., Wyszynska, A.,
707 Godlewska, R., and Jagusztyn-Krynicka, E.K. (2011). *Campylobacter jejuni dsb* gene expression
708 is regulated by iron in a Fur-dependent manner and by a translational coupling mechanism.
709 *Bmc Microbiology* 11, 16.

710 Graentzdoerffer, A., Rauh, D., Pich, A., and Andreesen, J.R. (2003). Molecular and biochemical
711 characterization of two tungsten- and selenium-containing formate dehydrogenases from
712 Eubacterium acidaminophilum that are associated with components of an iron-only
713 hydrogenase. *Arch Microbiol* 179, 116-130.

714 Grinnage-Pulley, T., Mu, Y., Dai, L., and Zhang, Q.J. (2016). Dual Repression of the Multidrug Efflux
715 Pump CmeABC by CosR and Cmer in *Campylobacter jejuni*. *Frontiers in Microbiology* 7.

716 Grinnage-Pulley, T., and Zhang, Q.J. (2015). Genetic Basis and Functional Consequences of
717 Differential Expression of the CmeABC Efflux Pump in *Campylobacter jejuni* Isolates. *Plos One*
718 10.

719 Guccione, E., Hitchcock, A., Hall, S.J., Mulholland, F., Shearer, N., Van Vliet, A.H.M., and Kelly, D.J.
720 (2010). Reduction of fumarate, mesaconate and crotonate by Mfr, a novel oxygen-regulated
721 periplasmic reductase in *Campylobacter jejuni*. *Environmental Microbiology* 12, 576-591.

722 Guyard-Nicodeme, M., Tresse, O., Houard, E., Jugiau, F., Courtillon, C., El Manaa, K., Laisney, M.J.,
723 and Chemaly, M. (2013). Characterization of *Campylobacter spp.* transferred from naturally
724 contaminated chicken legs to cooked chicken slices via a cutting board. *International Journal*
725 *of Food Microbiology* 164, 7-14.

726 Hald, B., Skov, M.N., Nielsen, E.M., Rahbek, C., Madsen, J.J., Waino, M., Chriel, M., Nordentoft, S.,
727 Baggesen, D.L., and Madsen, M. (2016). *Campylobacter jejuni* and *Campylobacter coli* in wild
728 birds on Danish livestock farms. *Acta Vet Scand* 58, 11.

729 Haldar, S., Gupta, A.J., Yan, X., Miličić, G., Hartl, F.U., and Hayer-Hartl, M. (2015). Chaperonin-Assisted
730 Protein Folding: Relative Population of Asymmetric and Symmetric GroEL:GroES Complexes.
731 *Journal of Molecular Biology* 427, 2244-2255.

732 Hayer-Hartl, M., Bracher, A., and Hartl, F.U. (2016). The GroEL-GroES Chaperonin Machine: A Nano-
733 Cage for Protein Folding. *Trends in Biochemical Sciences* 41, 62-76.

734 Hofreuter, D. (2014). Defining the metabolic requirements for the growth and colonization capacity
735 of *Campylobacter jejuni*. *Frontiers in Cellular and Infection Microbiology* 4.

736 Hue, O., Le Bouquin, S., Laisney, M.-J., Allain, V., Lalande, F., Petetin, I., Rouxel, S., Quesne, S.,
737 Gloaguen, P.-Y., Picherot, M., Santolini, J., Salvat, G., Bougeard, S., and Chemaly, M. (2010).
738 Prevalence of and risk factors for *Campylobacter spp.* contamination of broiler chicken
739 carcasses at the slaughterhouse. *Food Microbiology* 27, 992-999.

740 Huyer, M., Parr, T.R., Hancock, R.E.W., and Page, W.J. (1986). Outer-membrane porin protein of
741 *Campylobacter-jejuni*. *Fems Microbiology Letters* 37, 247-250.

742 Hwang, S., Zhang, Q.J., Ryu, S., and Jeon, B. (2012). Transcriptional Regulation of the CmeABC
743 Multidrug Efflux Pump and the KatA Catalase by CosR in *Campylobacter jejuni*. *Journal of*
744 *Bacteriology* 194, 6883-6891.

745 Inaba, K., and Ito, K. (2008). Structure and mechanisms of the DsbB-DsbA disulfide bond generation
746 machine. *Biochimica Et Biophysica Acta-Molecular Cell Research* 1783, 520-529.

747 Inaba, K., Murakami, S., Suzuki, M., Nakagawa, A., Yamashita, E., Okada, K., and Ito, K. (2006). Crystal
748 structure of the DsbB-DsbA complex reveals a mechanism of disulfide bond generation. *Cell*
749 127, 789-801.

750 Ito, K., and Inaba, K. (2008). The disulfide bond formation (Dsb) system. *Current Opinion in Structural*
751 *Biology* 18, 450-458.

752 Jardim-Messeder, D., Cabreira-Cagliari, C., Rauber, R., Turchetto-Zolet, A.C., Margis, R., and Margis-
753 Pinheiro, M. (2017). Fumarate reductase superfamily: A diverse group of enzymes whose

754 evolution is correlated to the establishment of different metabolic pathways. *Mitochondrion*
755 34, 56-66.

756 Jeon, B., and Zhang, Q.J. (2009). Sensitization of *Campylobacter jejuni* to fluoroquinolone and
757 macrolide antibiotics by antisense inhibition of the CmeABC multidrug efflux transporter.
758 *Journal of Antimicrobial Chemotherapy* 63, 946-948.

759 Kaakoush, N.O., Castano-Rodriguez, N., Mitchell, H.M., and Man, S.M. (2015). Global Epidemiology of
760 *Campylobacter* Infection. *Clin Microbiol Rev* 28, 687-720.

761 Kaakoush, N.O., Man, S.M., Lamb, S., Raftery, M.J., Wilkins, M.R., Kovach, Z., and Mitchell, H. (2010).
762 The secretome of *Campylobacter concisus*. *FEBS Journal* 277, 1606-1617.

763 Kalmokoff, M., Lanthier, P., Tremblay, T.L., Foss, M., Lau, P.C., Sanders, G., Austin, J., Kelly, J., and
764 Szymanski, C.M. (2006). Proteomic analysis of *Campylobacter jejuni* 11168 biofilms reveals a
765 role for the motility complex in biofilm formation. *Journal of Bacteriology* 188, 4312-4320.

766 Kanehisa, M., Sato, Y., Kawashima, M., Furumichi, M., and Tanabe, M. (2016). KEGG as a reference
767 resource for gene and protein annotation. *Nucleic Acids Res* 44, D457-462.

768 Klancnik, A., Botteldoorn, N., Herman, L., and Mozina, S.S. (2006). Survival and stress induced
769 expression of *groEL* and *rpoD* of *Campylobacter jejuni* from different growth phases.
770 *International Journal of Food Microbiology* 112, 200-207.

771 Lasserre, J.P., and Menard, A. (2012). Two-dimensional blue native/SDS gel electrophoresis of
772 multiprotein complexes. *Methods Mol Biol* 869, 317-337.

773 Li, Z.F., Lou, H.Q., Ojcius, D.M., Sun, A.H., Sun, D., Zhao, J.F., Lin, X.A., and Yan, J. (2014). Methyl-
774 accepting chemotaxis proteins 3 and 4 are responsible for *Campylobacter jejuni* chemotaxis
775 and jejuna colonization in mice in response to sodium deoxycholate. *Journal of Medical*
776 *Microbiology* 63, 343-354.

777 Lin, J., Akiba, M., Sahin, O., and Zhang, Q.J. (2005). CmeR functions as a transcriptional repressor for
778 the multidrug efflux pump CmeABC in *Campylobacter jejuni*. *Antimicrobial Agents and*
779 *Chemotherapy* 49, 1067-1075.

780 Lin, J., Michel, L.O., and Zhang, Q.J. (2002). CmeABC functions as a multidrug efflux system in
781 *Campylobacter jejuni*. *Antimicrobial Agents and Chemotherapy* 46, 2124-2131.

782 Lin, J., Sahin, O., Michel, L.O., and Zhang, O.J. (2003). Critical role of multidrug efflux pump CmeABC
783 in bile resistance and in vivo colonization of *Campylobacter jejuni*. *Infection and Immunity* 71,
784 4250-4259.

785 Lomize, M.A., Pogozheva, I.D., Joo, H., Mosberg, H.I., and Lomize, A.L. (2012). OPM database and
786 PPM web server: resources for positioning of proteins in membranes. *Nucleic Acids Res* 40,
787 D370-376.

788 Mace, S., Haddad, N., Zagorec, M., and Tresse, O. (2015). Influence of measurement and control of
789 microaerobic gaseous atmospheres in methods for *Campylobacter* growth studies. *Food*
790 *Microbiology* 52, 169-176.

791 Moore, J.E., Corcoran, D., Dooley, J.S.G., Fanning, S., Lucey, B., Matsuda, M., Mcdowell, D.A.,
792 Megraud, F., Millar, B.C., O'mahony, R., O'riordan, L., O'rourke, M., Rao, J.R., Rooney, P.J.,
793 Sails, A., and Whyte, P. (2005). *Campylobacter*. *Veterinary Research* 36, 351-382.

794 Motojima, F., and Yoshida, M. (2015). Productive folding of a tethered protein in the chaperonin
795 GroEL–GroES cage. *Biochemical and Biophysical Research Communications* 466, 72-75.

796 Nachamkin, I. (2002). Chronic effects of *Campylobacter* infection. *Microbes and Infection* 4, 399-403.

797 Okuno, D., Iino, R., and Noji, H. (2011). Rotation and structure of FoF1-ATP synthase. *Journal of*
798 *Biochemistry* 149, 655-664.

799 Parkhill, J., Wren, B.W., Mungall, K., Ketley, J.M., Churcher, C., Basham, D., Chillingworth, T., Davies,
800 R.M., Feltwell, T., Holroyd, S., Jagels, K., Karlyshev, A.V., Moule, S., Pallen, M.J., Penn, C.W.,
801 Quail, M.A., Rajandream, M.A., Rutherford, K.M., Van Vliet, A.H.M., Whitehead, S., and
802 Barrell, B.G. (2000). The genome sequence of the food-borne pathogen *Campylobacter jejuni*
803 reveals hypervariable sequences. *Nature* 403, 665-668.

804 Planas-Iglesias, J., Bonet, J., Garcia-Garcia, J., Marin-Lopez, M.A., Feliu, E., and Oliva, B. (2013).
805 Understanding protein-protein interactions using local structural features. *J Mol Biol* 425,
806 1210-1224.

807 Pryjma, M., Apel, D., Huynh, S., Parker, C.T., and Gaynor, E.C. (2012). FdhTU-Modulated Formate
808 Dehydrogenase Expression and Electron Donor Availability Enhance Recovery of
809 *Campylobacter jejuni* following Host Cell Infection. *Journal of Bacteriology* 194, 3803-3813.

810 Pyndiah, S., Lasserre, J.P., Menard, A., Claverol, S., Prouzet-Mauleon, V., Megraud, F., Zerbib, F., and
811 Bonneu, M. (2007). Two-dimensional blue native/SDS gel electrophoresis of multiprotein
812 complexes from *Helicobacter pylori*. *Molecular & Cellular Proteomics* 6, 193-206.

813 Rastogi, V.K., and Girvin, M.E. (1999). Structural changes linked to proton translocation by subunit c
814 of the ATP synthase. *Nature* 402, 263-268.

815 Reisinger, V., and Eichacker, L.A. (2006). Analysis of membrane protein complexes by blue native
816 PAGE. *Proteomics*, 6-15.

817 Reisinger, V., and Eichacker, L.A. (2007). How to analyze protein complexes by 2D blue native SDS-
818 PAGE. *Proteomics* 7 Suppl 1, 6-16.

819 Reisinger, V., and Eichacker, L.A. (2008). Solubilization of membrane protein complexes for blue
820 native PAGE. *Journal of Proteomics* 71, 277-283.

821 Robinson, D.A. (1981). Infective dose of *Campylobacter jejuni* in milk. *British Medical Journal* 282,
822 1584-1584.

823 Rodrigues, R.C., Haddad, N., Chevret, D., Cappelier, J.M., and Tresse, O. (2016). Comparison of
824 Proteomics Profiles of *Campylobacter jejuni* Strain Bf under Microaerobic and Aerobic
825 Conditions. *Frontiers in Microbiology* 7.

826 Rothery, R.A., Seime, A.M., Spiers, A.M.C., Maklashina, E., Schroder, I., Gunsalus, R.P., Cecchini, G.,
827 and Weiner, J.H. (2005). Defining the Q(P)-site of *Escherichia coli* fumarate reductase by site-
828 directed mutagenesis, fluorescence quench titrations and EPR spectroscopy. *Febs Journal*
829 272, 313-326.

830 Sachs, J.N., and Engelman, D.M. (2006). "Introduction to the membrane protein reviews: The
831 interplay of structure, dynamics, and environment in membrane protein function," in *Annual*
832 *Review of Biochemistry*.), 707-712.

833 Schägger, H. (2002). Respiratory chain supercomplexes of mitochondria and bacteria. *Biochimica et*
834 *Biophysica Acta (BBA) - Bioenergetics* 1555, 154-159.

835 Schagger, H., and Von Jagow, G. (1991). Blue native electrophoresis for isolation of membrane
836 protein complexes in enzymatically active form. *Analytical Biochemistry* 199, 223-231.

837 Scott, N.E., Marzook, N.B., Cain, J.A., Solis, N., Thaysen-Andersen, M., Djordjevic, S.P., Packer, N.H.,
838 Larsen, M.R., and Cordwell, S.J. (2014). Comparative Proteomics and Glycoproteomics Reveal
839 Increased N-Linked Glycosylation and Relaxed Sequon Specificity in *Campylobacter jejuni*
840 NCTC11168 O. *Journal of Proteome Research* 13, 5136-5150.

841 Scott, N.E., Parker, B.L., Connolly, A.M., Paulech, J., Edwards, A.V.G., Crossett, B., Falconer, L.,
842 Kolarich, D., Djordjevic, S.P., Hojrup, P., Packer, N.H., Larsen, M.R., and Cordwell, S.J. (2011).
843 Simultaneous Glycan-Peptide Characterization Using Hydrophilic Interaction
844 Chromatography and Parallel Fragmentation by CID, Higher Energy Collisional Dissociation,
845 and Electron Transfer Dissociation MS Applied to the N-Linked Glycoproteome of
846 *Campylobacter jejuni*. *Molecular & Cellular Proteomics* 10.

847 Seal, B.S., Hiatt, K.L., Kuntz, R.L., Woolsey, R., Schegg, K.M., Ard, M., and Stintzi, A. (2007). Proteomic
848 analyses of a robust versus a poor chicken gastrointestinal colonizing isolate of
849 *Campylobacter jejuni*. *J Proteome Res* 6, 4582-4591.

850 Shaw, F.L., Mulholland, F., Le Gall, G., Porcelli, I., Hart, D.J., Pearson, B.M., and Van Vliet, A.H.M.
851 (2012). Selenium-Dependent Biogenesis of Formate Dehydrogenase in *Campylobacter jejuni*
852 Is Controlled by the fdhTU Accessory Genes. *Journal of Bacteriology* 194, 3814-3823.

853 Silva, J., Leite, D., Fernandes, M., Mena, C., Gibbs, P.A., and Teixeira, P. (2011). *Campylobacter spp.* as
854 a foodborne pathogen: a review. *Frontiers in Microbiology* 2.

855 Smart, J.P., Cliff, M.J., and Kelly, D.J. (2009). A role for tungsten in the biology of *Campylobacter*
856 *jejuni*: tungstate stimulates formate dehydrogenase activity and is transported via an ultra-
857 high affinity ABC system distinct from the molybdate transporter. *Molecular Microbiology* 74,
858 742-757.

859 Sohn, S.H., and Lee, Y.C. (2011). The genome-wide expression profile of gastric epithelial cells
860 infected by naturally occurring cagA isogenic strains of *Helicobacter pylori*. *Environmental*
861 *Toxicology and Pharmacology* 32, 382-389.

862 Sperling, L.J., Tang, M., Berthold, D.A., Nesbitt, A.E., Gennis, R.B., and Rienstra, C.M. (2013). Solid-
863 State NMR Study of a 41 kDa Membrane Protein Complex DsbA/DsbB. *Journal of Physical*
864 *Chemistry B* 117, 6052-6060.

865 Stephen, K.B., Helen, M.B., Cole, C., Jose, M.D., Zukang, F., John, W., Jasmine, Y., and Christine, Z.
866 (2018). RCSB Protein Data Bank: Sustaining a living digital data resource that enables
867 breakthroughs in scientific research and biomedical education. *Protein Science* 27, 316-330.

868 Sulaeman, S., Hernould, M., Schaumann, A., Coquet, L., Bolla, J.M., De, E., and Tresse, O. (2012).
869 Enhanced adhesion of *Campylobacter jejuni* to abiotic surfaces is mediated by membrane
870 proteins in oxygen-enriched conditions. *PLoS One* 7.

871 Szklarczyk, D., Morris, J.H., Cook, H., Kuhn, M., Wyder, S., Simonovic, M., Santos, A., Doncheva, N.T.,
872 Roth, A., Bork, P., Jensen, L.J., and Von Mering, C. (2017). The STRING database in 2017:
873 quality-controlled protein-protein association networks, made broadly accessible. *Nucleic*
874 *Acids Res* 45, D362-d368.

875 Tresse, O. (2017). *Proteomics Analyses Applied to the Human Foodborne Bacterial Pathogen*
876 *Campylobacter spp.*

877 Turonova, H., Briandet, R., Rodrigues, R., Hernould, M., Hayek, N., Stintzi, A., Pazlarova, J., and
878 Tresse, O. (2015). Biofilm spatial organization by the emerging pathogen *Campylobacter*
879 *jejuni*: comparison between NCTC 11168 and 81-176 strains under microaerobic and oxygen-
880 enriched conditions. *Frontiers in Microbiology* 6.

881 Turonova, H., Haddad, N., Hernould, M., Chevret, D., Pazlarova, J., and Tresse, O. (2017). Profiling of
882 *Campylobacter jejuni* Proteome in Exponential and Stationary Phase of Growth. *Frontiers in*
883 *Microbiology* 8.

884 Vallenet, D., Calteau, A., Cruveiller, S., Gachet, M., Lajus, A., Josso, A., Mercier, J., Renaux, A., Rollin,
885 J., Rouy, Z., Roche, D., Scarpelli, C., and Medigue, C. (2017). MicroScope in 2017: an
886 expanding and evolving integrated resource for community expertise of microbial genomes.
887 *Nucleic Acids Research* 45, D517-D528.

888 Wai, S.N., Nakayama, K., Umene, K., Moriya, T., and Amako, K. (1996). Construction of a ferritin-
889 deficient mutant of *Campylobacter jejuni*: contribution of ferritin to iron storage and
890 protection against oxidative stress. *Molecular Microbiology* 20, 1127-1134.

891 Watson, E., Sherry, A., Inglis, N.F., Lainson, A., Jyothi, D., Yaga, R., Manson, E., Imrie, L., Everest, P.,
892 and Smith, D.G. (2014). Proteomic and genomic analysis reveals novel *Campylobacter jejuni*
893 outer membrane proteins and potential heterogeneity. *EuPA Open Proteom* 4, 184-194.

894 Weerakoon, D.R., Borden, N.J., Goodson, C.M., Grimes, J., and Olson, J.W. (2009). The role of
895 respiratory donor enzymes in *Campylobacter jejuni* host colonization and physiology.
896 *Microbial Pathogenesis* 47, 8-15.

897 Weerakoon, D.R., and Olson, J.W. (2008). The *Campylobacter jejuni* NADH : Ubiquinone
898 oxidoreductase (complex I) utilizes flavodoxin rather than NADH. *Journal of Bacteriology* 190,
899 915-925.

900 Weingarten, R.A., Taveirne, M.E., and Olson, J.W. (2009). The Dual-Functioning Fumarate Reductase
901 Is the Sole Succinate: Quinone Reductase in *Campylobacter jejuni* and Is Required for Full
902 Host Colonization. *Journal of Bacteriology* 191, 5293-5300.

903 Wetie, A., Sokolowska, I., Woods, A., Roy, U., Loo, J., and Darie, C. (2013). Investigation of stable and
904 transient protein-protein interactions: Past, present, and future. *PROTEOMICS* 13, 538-557.

905 Wohlbrand, L., Ruppertsberg, H.S., Feenders, C., Blasius, B., Braun, H.P., and Rabus, R. (2016). Analysis
906 of membrane-protein complexes of the marine sulfate reducer *Desulfobacula toluolica* Tol2

907 by 1D blue native-PAGE complexome profiling and 2D blue native-/SDS-PAGE. *Proteomics* 16,
908 973-988.

909 Wu, W.H., Tran-Gyamfi, M.B., Jaryenneh, J.D., and Davis, R.W. (2016). Cofactor engineering of ketol-
910 acid reductoisomerase (IlvC) and alcohol dehydrogenase (YqhD) improves the fusel alcohol
911 yield in algal protein anaerobic fermentation. *Algal Research-Biomass Biofuels and*
912 *Bioproducts* 19, 162-167.

913 Yan, M.G., Sahin, O., Lin, J., and Zhang, Q.J. (2006). Role of the CmeABC efflux pump in the
914 emergence of fluoroquinolone-resistant *Campylobacter* under selection pressure. *Journal of*
915 *Antimicrobial Chemotherapy* 58, 1154-1159.

916 You, Y., He, L., Zhang, M., Fu, J., Gu, Y., Zhang, B., Tao, X., and Zhang, J. (2012). Comparative genomics
917 of *Helicobacter pylori* strains of China associated with different clinical outcome. *PLoS One* 7,
918 e38528.

919 Young, J.Y., Westbrook, J.D., Feng, Z.K., Peisach, E., Persikova, I., Sala, R., Sen, S., Berrisford, J.M.,
920 Swaminathan, G.J., Oldfield, T.J., Gutmanas, A., Igarashi, R., Armstrong, D.R., Baskaran, K.,
921 Chen, L., Chen, M.Y., Clark, A.R., Di Costanzo, L., Dimitropoulos, D., Gao, G.H., Ghosh, S.,
922 Gore, S., Guranovic, V., Hendrickx, P.M.S., Hudson, B.P., Ikegawa, Y., Kengaku, Y., Lawson,
923 C.L., Liang, Y.H., Mak, L., Mukhopadhyay, A., Narayanan, B., Nishiyama, K., Patwardhan, A.,
924 Sahni, G., Sanz-Garcia, E., Sato, J., Sekharan, M.R., Shao, C.H., Smart, O.S., Tan, L.H., Van
925 Ginkel, G., Yang, H.W., Zhuravleva, M.A., Markley, J.L., Nakamura, H., Kurisu, G., Kleywegt,
926 G.J., Velankar, S., Berman, H.M., and Burley, S.K. (2018). Worldwide Protein Data Bank
927 biocuration supporting open access to high-quality 3D structural biology data. *Database-the*
928 *Journal of Biological Databases and Curation*.

929 Yum, S., Xu, Y., Piao, S., Sim, S., Kim, H., Jo, W., Kim, K., Kweon, H., Jeong, M., Jeon, H., Lee, K., and
930 Ha, N. (2009). Crystal Structure of the Periplasmic Component of a Tripartite Macrolide-
931 Specific Efflux Pump. *Journal of Molecular Biology* 387, 1286-1297.

932 Zautner, A.E., Tareen, A.M., Groß, U., and Lugert, R. (2012). Chemotaxis in *Campylobacter jejuni*.
933 *European Journal of Microbiology & Immunology* 2, 24-31.

934 Zhang, Q.J., Meitzler, J.C., Huang, S.X., and Morishita, T. (2000). Sequence polymorphism, predicted
935 secondary structures, and surface-exposed conformational epitopes of *Campylobacter* major
936 outer membrane protein. *Infection and Immunity* 68, 5679-5689.

937 Zommiti, M., Almohammed, H., and Ferchichi, M. (2016). Purification and Characterization of a Novel
938 Anti-*Campylobacter* Bacteriocin Produced by *Lactobacillus curvatus* DN317. *Probiotics and*
939 *Antimicrobial Proteins* 8, 191-201.

940

941 **Figure Legends**

942 **Fig 1. Separation of membrane protein complexes from *C. jejuni* strain 81-176 by BN-**
943 **PAGE.** 10 µg (A) and 20 µg (B) of membrane protein complexes were solubilized with DDM
944 at concentrations ranging from 1, 2 and 5% (w/v). Mass marker are indicated in the central
945 lane (MW in kDa).

946 **Fig 2. 2D-BN/SDS-PAGE separation of membrane protein complexes of *C. jejuni* 81-**
947 **176.** Acrylamide gradient was 4-18% for BN-PAGE and acrylamide concentration was 10%
948 for SDS-PAGE. Mass markers for BN-PAGE and SDS-PAGE are respectively indicated at
949 the top left side of the gel. Proteins identified by LC-MS/MS are indicated by **blue arrows**.
950 Proteins that do not reach identification criteria after LC-MS/MS analysis are indicated with
951 **black arrows**. First numbers correspond to complexes and second numbers to subunits of
952 these complexes.

953 **Fig 3. Membrane protein complexes identified by 2-D BN/SDS-PAGE in *C. jejuni* 81-**
954 **176.** Colour of complexes corresponds to their function in cell: Green for molecules
955 trafficking, Red for protein biosynthesis and folding, Blue for respiration, Yellow for motility
956 and Orange for the oxidative phosphorylation.

957 **Fig 4. Phylogenetic tree of proteins belonging to efflux pumps CmeABC and**
958 **MacABputC.** Alignment was performed using MAFFT (GeneiousR9) with functional
959 domain and protein structure (Phylus) in 14 *C. jejuni* strains and 6 *C. coli* strains. Bootstraps
960 percentages were added to internal branches for 1000 replicates. **Strains used in this study are**
961 **listed in Table S2.**

962 **Fig 5. Consensus sequence logo of CosR-binding box of the upstream sequences of genes**
963 **with CosR-binding capacity (*cmeA* and *macA*).** Consensus sequence logo of CosR-binding
964 box defined by Turonova *et al.*, 2017 (A) alignment of upstream sequences of *cmeA* and

965 macA by Geneious 9.1.8 (B) Consensus sequence logo of CosR-binding box redefined (C).
966 w-A or T; y-C or T; m-A or C and k-G or T.

967 **Fig 6. Distribution of CmeABC and MacABputC subunits in bacteria using Blastp with**
968 ***C. jejuni* 81-176 protein sequences of each subunit as queries in RefSeq_protein**
969 **database. The data are based on the hits presented in Table S3.**

970 Legend of figures in Supplementary data

971 **Figure S1. Homemade strips in 5 steps to separate the subunits of protein complexes**
972 **in a reproducing manner.** A- Cut the strip with a clean glass plate following the well
973 where the sample was deposited, equilibrate the gel lane in DTT and iodoacetamide
974 buffers as indicated in material and methods; B- lay the gel strip on the wet plastic support
975 using clean forceps; C- Stick the plastic face of the strip on the glass behind; D- Slide the
976 strip until touching the precast polyacrylamide gel; E- Fill the gap and overlaid the strip
977 with low melting agarose using a sterile syringe.

978 **Figure S2. 2D-BN-SDS-PAGE profiling before (A) and after optimization (B) of**
979 **protein complexes and their subunit separation.** The first dimension for complex
980 separation was performed on 4 to 18% acrylamide gradient gels with 2% Dodecyl- β -D-
981 Maltoside (DDM).

982 **Figure S3. 2D-BN/SDS-PAGE western blot, using antibody anti-MOMP (A) and**
983 **antibody anti-CadF (B).** The image in the middle corresponds to the identified proteins
984 complexes before the Western-blot The black arrow indicate the identified proteins with
985 anti-PorA antibody and the white arrow the identify protein with anti-CadF antibody on
986 the 2D-BN/SDS-PAGE.

987

988 **Table 1. Description of membrane protein complexes identified in *C. jejuni* strain 81-176**
 989 **using two-dimensional BN/SDS-PAGE.**

Complex function	complex ID	Spot ID	Access No. (NCBI)	Protein ID	Gene name	Mascot score (a)	NPM/PC (%) (b)	pI/MW (kDa) (theoretical)	
Oxidative phosphorylation	2	2.1	EAQ73056.1	Fumarate reductase flavoprotein subunit	<i>frdA</i>	413	12/20	6.36/74	
		2.2	EAQ73378.1	Fumarate reductase iron-sulfur subunit	<i>frdB</i>	153	4/22	5.37/27	
		2.3	EAQ73136.1	Fumarate reductase cytochrome b-556 subunit	<i>frdC</i>	38	2*/5	9.37/30	
		9.1	EAQ72593.1	Cytochrome c oxidase, cbb3-type, subunit II	<i>ccoO</i>	136	4/23	5.86/25	
		11.1	EAQ71910.1	FOF1 ATP synthase subunit beta	<i>atpD</i>	102	2/5	4.97/51	
		19.1	EAQ72569.1	NADH dehydrogenase subunit G	<i>nuoG</i>	205	6/9	5.49/93	
		19.2	EAQ72908.1	NADH dehydrogenase subunit D	<i>nuoD</i>	121	3/7	5.51/47	
		19.3	EAQ72659.1	NADH dehydrogenase subunit C	<i>nuoC</i>	131	2/10	7.77/31	
Respiration	8	8.1	EAQ72956.1	Formate dehydrogenase, alpha unit, selenocysteine-containing	<i>fdhA</i>	401	12/19	6.09/83	
		8.2	EAQ72781.1	Formate dehydrogenase, iron-sulfur subunit	<i>fdhB</i>	65	2*/9	5.99/24	
		12.1	EAQ72716.1	Quinone-reactive Ni/Fe-hydrogenase, large subunit	<i>hydB</i>	98	2/6	6.26/64	
		12.2	EAQ72716.1	Quinone-reactive Ni/Fe-hydrogenase, large subunit	<i>hydB</i>	164	6/14	6.26/64	
Protein biosynthesis and folding	0	0	EAQ72817.1	Chaperonin GroEL	<i>groEL</i>	698	16/39	5.02/58	
		4.1	EAQ71919.1	DsbB family disulfide bond formation protein	<i>dsbB</i>	139	3/7	8.57/57	
		10.1	EAQ73315.1	Penicillin-binding protein 1A	<i>pbpA</i>	81	3/5	8.35/73	
		10.2	EAQ73158.1	Methyl-accepting chemotaxis protein	<i>CJJ_0180</i>	101	3/5	4.94/73	
		10.3	EAQ73158.1	Methyl-accepting chemotaxis protein	<i>CJJ_0180</i>	132	4/6	4.94/73	
Efflux pumps, virulence and molecules trafficking	3	3.1	EAQ72728.1	Major outer membrane protein	<i>porA**</i>	2004	14/49	4.72/46	
		3.2	EAQ72728.1	Major outer membrane protein	<i>porA**</i>	1989	14/48	4.72/46	
		3.3	EAQ72728.1	Major outer membrane protein	<i>porA**</i>	1133	8/30	4.72/46	
	5	5.1	EAQ73202.1	Outer membrane protein	<i>bamA</i>	70	2*/4	5.57/83	
		5.2	EAQ72997.1	Conserved hypothetical protein (putative lipoprotein)	<i>CJJ_0419</i>	196	5/17	8.48/37	
	6	6.1	EAQ73082.1	RND efflux system, outer membrane lipoprotein CmeC	<i>cmeC</i>	129	7/10	5.14/55	
		6.2	EAQ73146.1	RND efflux system, inner membrane transporter CmeB	<i>cmeB</i>	101	2/2	6.48/114	
		6.3	EAQ73146.1	RND efflux system, inner membrane transporter CmeB	<i>cmeB</i>	121	2/2	6.48/114	
	13	13.1	EAQ72976.1	RND efflux system, membrane fusion protein CmeA	<i>cmeA</i>	102	3/10	8.29/40	
		13.1	EAQ72728.1	Major outer membrane protein	<i>porA**</i>	231	4/11	4.72/46	
		13.2	EAQ72728.1	Major outer membrane protein	<i>porA**</i>	419	10/30	4.72/46	
		15.1	EAQ72952.1	Capsular polysaccharide ABC transporter	<i>kpsE</i>	136	3/8	6.22/43	
		15.2	EAQ72738.1	Outer membrane fibronectin-binding protein	<i>cadF**</i>	55	2/8	5.89/36	
		20.1	EAQ73027.1	Macrolide-specific efflux protein macB	<i>CJJ_0636</i>	35	2*/1	9.25/70	
	18	18.1	EAQ72087.1	CjaA protein	<i>cjaA</i>	21	1/4	5.69/31	
		18.2	EAQ72374.1	CjaC protein	<i>cjaC</i>	250	6/25	6.48/28	
	Mobility	17	17.1	EAQ72823.1	Flagellar basal body-associated protein FliL	<i>fliL</i>	47	1/15	4.93/20
	Unknown	1	1.1	EAQ73148.1	Ketol acid reductoisomerase	<i>ilvC</i>	365	8/27	6.1/37
1.2			EAQ72988.1	Nonheme iron-containing ferritin	<i>ftn</i>	73	2/16	5.34/20	
14		14.1	EAQ73158.1	Methyl-accepting chemotaxis protein	<i>CJJ_0180</i>	94	2/4	4.94/73	
		14.2	EAQ73158.1	Methyl-accepting chemotaxis protein	<i>CJJ_0180</i>	111	4/6	4.94/73	
Other	16	16.1	EAQ73030.1	Elongation factor Tu	<i>tuf</i>	60	2/8	5.11/44	

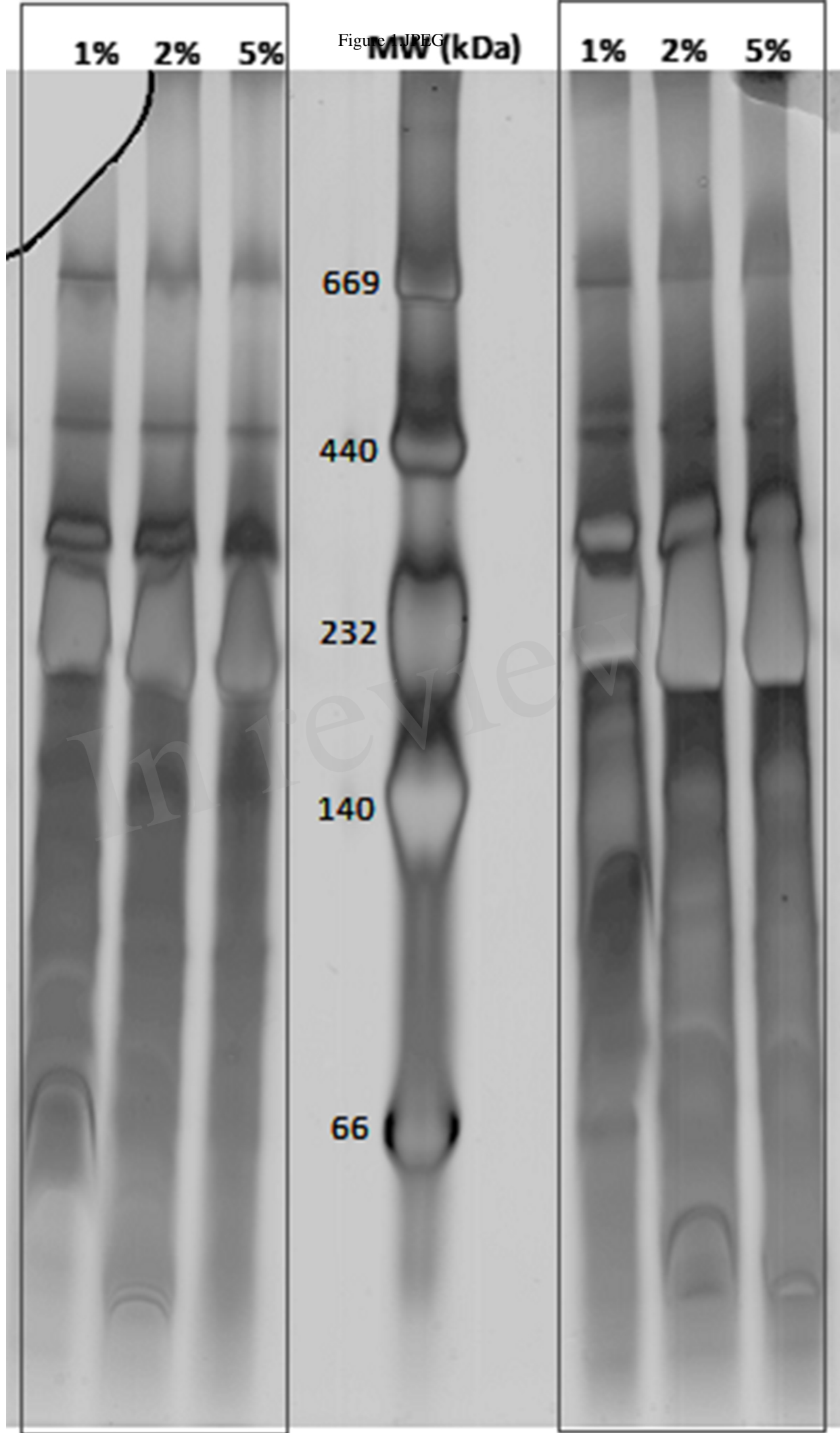
990

991 None of the proteins from the complex no. 7 have been identified.

992 (a) From all identified peptides (b) Peptides with only a significant individual ion score were considered for NPM (Number of Peptide Match) and PC (Protein Coverage). * One peptide with a non-significant score but mainly identified from y and b ions (see MS/MS fragmentation in supplementary data) are included to validate the identification. **proteins verified by Western Blot

996

997



A

B

Figure 2.JPEG

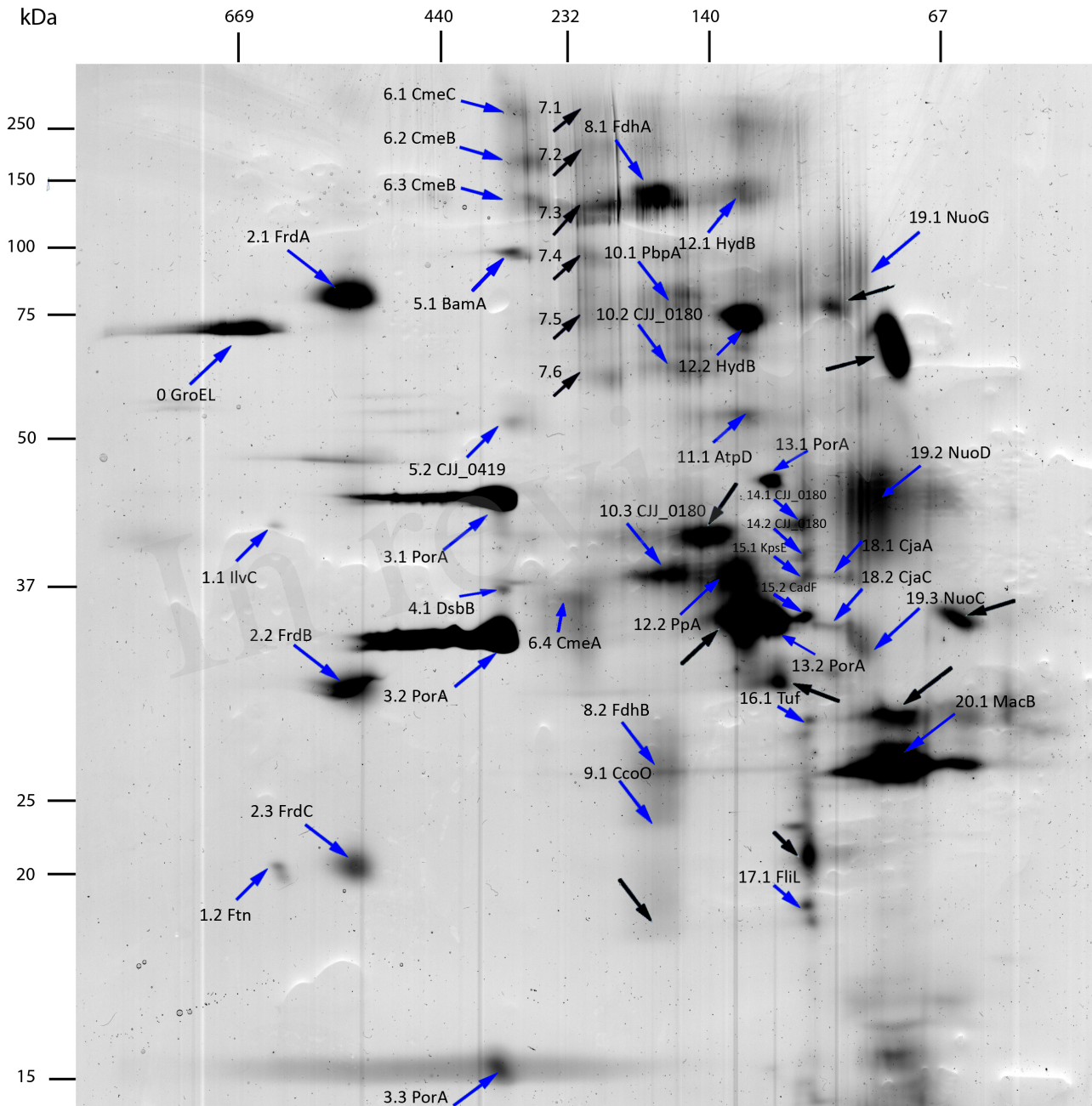


Figure 3.JPEG

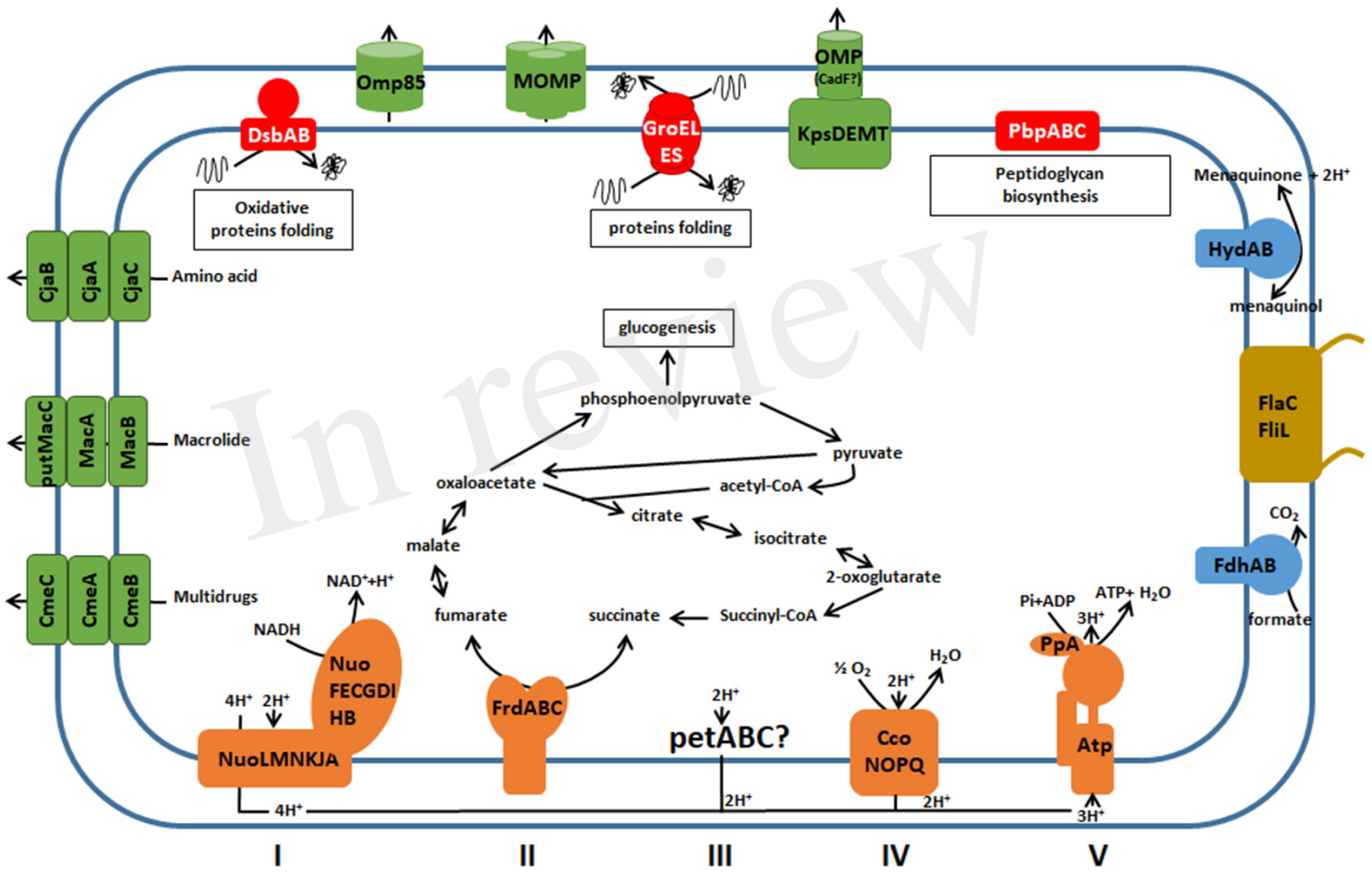


Figure 4.JPEG

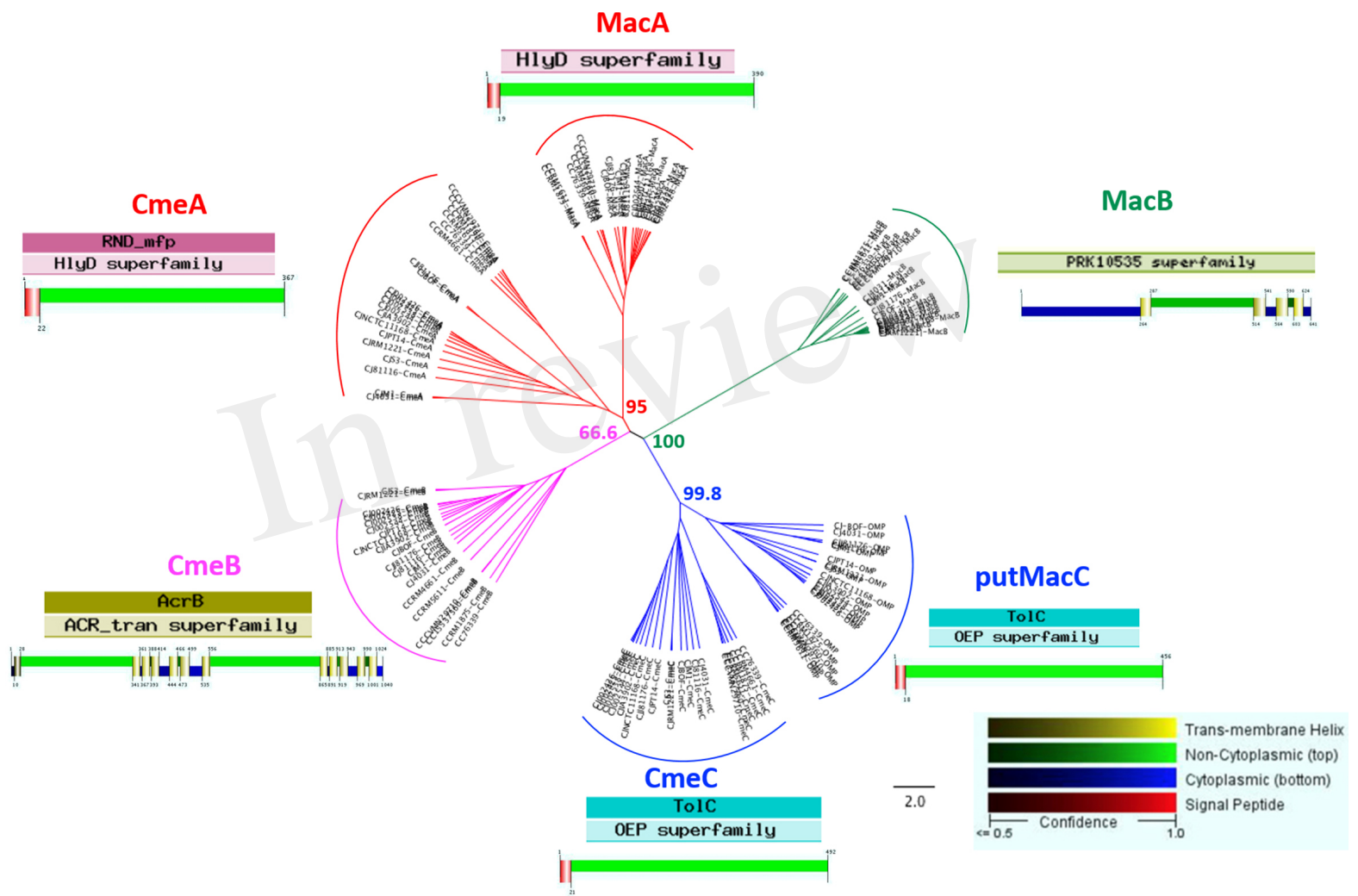


Figure 6.JPEG

